# Chapter 8. Carbon Burial, Transport, and Emission from Inland Aquatic Ecosystems in Alaska

By Sarah Stackpoole,[1] David Butman,[1,2] David Clow,[1] Kris Verdin,[1] Ben Gaglioti,[1,3] and Robert Striegl[1]

## 8.1. Highlights

- The total estimated surface area of inland waters in Alaska was approximately 60,000 square kilometers ($km^2$), which represents nearly 3.5 percent of the total land surface area.
- The total net estimated carbon flux (coastal export plus carbon dioxide [$CO_2$] emissions from rivers and lakes minus burial in lake sediments) from inland waters of Alaska was 41.2 teragrams of carbon per year (TgC/yr) (5th and 95th percentiles of 30.4 TgC/yr and 59.7 TgC/yr). Total carbon yield based on total land surface area was 27.5 grams of carbon per square meter per year ($gC/m^2/yr$) (5th and 95th percentiles of 20.1 $gC/m^2/yr$ and 39.5 $gC/m^2/yr$).
- Riverine systems of Alaska functioned as carbon sources to coastal ecosystems and the atmosphere. Dissolved inorganic carbon and total organic carbon exports to coastal areas were 12.2 $gC/m^2/yr$ (5th and 95th percentiles of 10.8 $gC/m^2/yr$ and 16.6 $gC/m^2/yr$) and $CO_2$ emissions to the atmosphere were 11.0 $gC/m^2/yr$ (5th and 95th percentiles of 6.0 $gC/m^2/yr$ and 17.4 $gC/m^2/yr$).
- Lacustrine systems acted as both sources and sinks of carbon with 5.5 $gC/m^2/yr$ (5th and 95th percentiles of 4.0 $gC/m^2/yr$ and 7.4 $gC/m^2/yr$) emitted as $CO_2$ to the atmosphere and –1.2 $gC/m^2/yr$ (5th and 95th percentiles of –0.7 $gC/m^2/yr$ and –1.9 $gC/m^2/yr$) of organic carbon buried in lake sediments. Negative values represent sequestration.
- There was considerable variability in the estimated carbon fluxes of inland waters among the six hydrologic regions in Alaska. This was due to the differences in the size and abundance of water bodies, topography, climate, land cover, permafrost, and glacier extent associated with each region.

## 8.2. Introduction

Section 712 of the Energy Independence and Security Act (EISA) of 2007 required an assessment of carbon fluxes related to freshwater aquatic ecosystems, including rivers and lakes, which collectively are categorized as inland waters. Carbon fluxes associated with aquatic ecosystems (this chapter) are assessed separately from those of the terrestrial ecosystems (chapters 6 and 7) in this report because of limited empirical aquatic data and a lack of a large-scale, spatially explicit carbon model that integrates terrestrial and aquatic fluxes.

Inland aquatic ecosystems are critical components of the carbon cycle. Rivers and lakes serve as sites for biogeochemical carbon reactions that result in an exchange of carbon dioxide ($CO_2$) among aquatic and terrestrial environments and the atmosphere, and rivers act as conduits that deliver carbon to the coast (Kling and others, 1992; Striegl and others, 2012; Tank, Raymond, and others, 2012; Crawford and others, 2013; McClelland and others, 2014; Sepulveda-Jauregui and others, 2014). Carbon sequestration in lake sediments may offset fluxes to oceans and the atmosphere (Naidu and others, 1999; Walter Anthony and others, 2014). Collectively, the amount of carbon moving through, into, and out of aquatic ecosystems makes them a significant component of carbon budgets at local, regional, and global scales (Cole and others, 2007;

[1]U.S. Geological Survey, Denver, Colo.

[2]University of Washington, Seattle, Wash.

[3]University of Alaska-Fairbanks, Fairbanks, Alaska.

Tranvik and others, 2009; Aufdenkampe and others, 2011; Butman and Raymond, 2011; Crawford and others, 2013; Raymond and others, 2013).

The objective of this chapter is to provide baseline estimates of aquatic carbon fluxes from inland waters for the six main hydrologic regions of Alaska: the Arctic Slope (called North Slope in this report), Northwest, Yukon, Southwest, South-Central, and Southeast (Seaber and others, 1987) (fig. 8.1).

These regions were chosen as the reporting units because, unlike the Alaska Landscape Conservation Cooperatives used in previous chapters of this report, the boundaries of the hydrologic regions coincide with natural drainage areas for rivers within the State. By leveraging existing hydrologic and carbon chemistry datasets, we estimated the following aquatic carbon fluxes: (1) lateral transport of dissolved inorganic carbon (DIC) and total organic carbon (TOC, composed of dissolved and particulate phases) from riverine systems to the coast, (2) gaseous carbon emissions of $CO_2$ from riverine systems, (3) gaseous carbon emissions of $CO_2$ from lacustrine systems, and (4) carbon burial in sediments of lakes. Aquatic flux values presented in this chapter were normalized to total land surface area to produce yield estimates, and comparisons of regional variability among yields are presented. Given the vulnerability of carbon stored in the soils and permafrost of Alaska to a warming climate and the strong linkages between terrestrial and aquatic ecosystems, it is important to provide accurate estimates of current carbon fluxes in aquatic environments, so that future climate change effects can be determined.

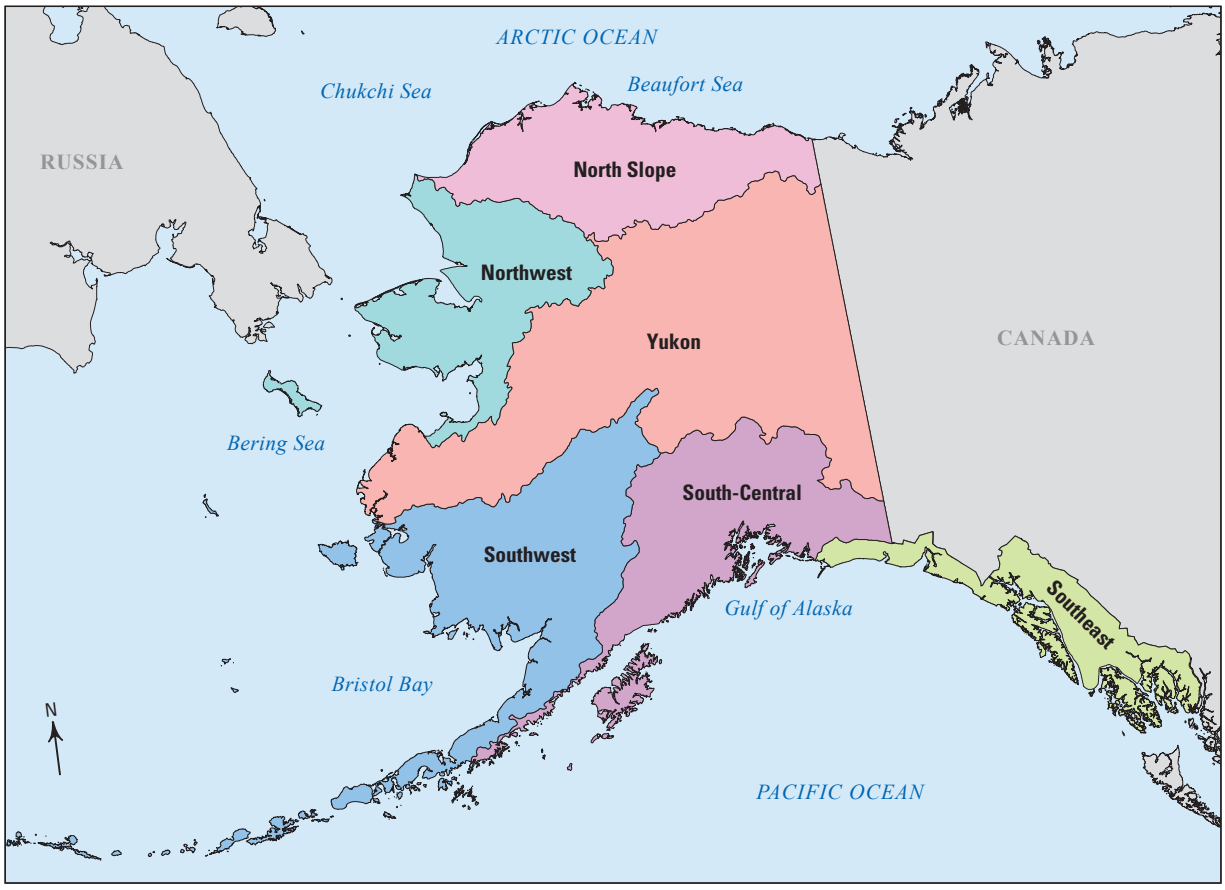


**Figure 8.1.** The six major hydrologic regions of Alaska: the Arctic Slope, called North Slope in this report, Northwest, Yukon, Southwest, South-Central, and Southeast from Seaber and others (1987).

## 8.3. Methods and Data

### 8.3.1. Physiography of Alaska Related to Inland Waters

The regional hydrology of Alaska is influenced by the State's varied physiography. The North Slope hydrologic region is characterized largely by an arctic coastal plain, which is poorly drained and dominated by dune-trough (Jorgenson and Shur, 2007) and thermokarst (Frohn and others, 2005) lakes. This region is underlain mostly by continuous permafrost (Jorgenson and others, 2008; Schuur and others, 2008). The Colville, Kuparuk, and Sagavanirktok Rivers, the largest rivers in the region, drain from the northern slope of the Brooks Range into the Beaufort Sea (fig. 8.2). The mountains in the Northwest hydrologic region have small pockets of glaciers and lakes at higher elevations (Wahrhaftig, 1965). Scattered lakes occur in lower elevation areas embedded in multiple sequences representing the late-Pleistocene (Hamilton, 1982) and Holocene glacial advances (Ellis and Calkin, 1984). The Kobuk and Noatak Rivers, the major rivers of the Northwest region, drain into the Chukchi Sea.

The intermontane plateau, commonly known as interior Alaska, occurs between the Brooks Range and the coastal mountain ranges of the Gulf of Alaska, and constitutes the Yukon hydrologic region. This region is underlain by discontinuous permafrost (Jorgenson and others, 2008; Schuur and


**Figure 8.2.** Coastal receiving waters and mountain ranges in the State of Alaska. Letters indicate major rivers: A, Unuk; B, Stikine; C, Taku; D, Alsek; E, Copper; F, Susitna; G, Nushagak; H, Kuskokwim; I, Yukon; J, Kobuk; K, Noatak; L, Colville; M, Kuparuk; and N, Sagavanirktok.

others, 2008) and, outside of the Brooks and Alaska Ranges, most of this region has never been glaciated. The Yukon River (3,340-kilometer [km] long) flows through this region to the Bering Sea and is the largest free-flowing river in the world. In the lowland areas near the Yukon River, there are areas with high density of lake coverage (Williams, 1962; Patton and Miller, 1970; Patton, 1973). The southwestern part of the intermontane plateau (the Southwest hydrologic region), is underlain by discontinuous, sporadic, and isolated permafrost (Jorgenson and others, 2008). Lowland areas contain many morainal lakes. Many large lakes occur in this region, and Lake Iliamna is the largest of these with a surface area of 2,600 square kilometers ($km^2$). The major rivers are the Nushagak River, which drains into Bristol Bay, and the Kuskokwim River, which drains to Kuskokwim Bay on the Bering Sea.

In the South-Central hydrologic region, the coastal mountain ranges contribute meltwater that is the dominant flow to the Susitna and Copper Rivers, which empty into the Cook Inlet and the Gulf of Alaska, respectively. The area is underlain by discontinuous and sporadic permafrost, and the mountainous areas contain glaciated regions, where many lakes are found in the ice-carved bedrock basins (Wahrhaftig, 1965). In the Southeast hydrologic region, short meltwater streams contribute a large volume of flow to the Gulf of Alaska. Larger transboundary rivers, including the Stikine, Taku, and Unuk Rivers, originate in the coastal mountain forests of Canada and contribute to the large volumes of flow in this region. The high-elevation mountains in this region have few lakes, but at lower elevations, rock-basin, cirque, and proglacial fjord lakes are abundant.

## 8.3.2. Estimating River Discharge, Watershed Area, and Lake Area

Estimates of mean annual discharge for the entire State of Alaska were made by applying previously developed regional regression equations (Parks and Madison, 1985), whereas the underlying framework, which provided the stream network and connectivity, was developed using the Elevation Derivatives for National Applications (EDNA) database (Verdin, 2000; Kost and others, 2002). The regional regression equations take the form of equation 8.1:

$$Q=(10a)\times(DAb)\times(Pc) \quad (8.1)$$

where

$Q$ is the mean annual streamflow, in cubic meters per second ($m^3/s$),

$DA$ is the drainage area, in $km^2$,

$P$ is the precipitation, in meters (m), and

$a$, $b$, and $c$ are regression parameters that vary by hydrologic regions.

Equation 8.1 was evaluated in a raster environment for every location (pixel) within the State of Alaska. Inputs to equation 8.1 for mean annual streamflow were derived from two main data sources: (1) Drainage area was derived from the EDNA layers, with necessary adjustments to account for drainage from Canada. The area was represented in the flow accumulation values associated with each pixel, converted to square kilometers. (2) The precipitation data used to evaluate equation 8.1 were historical monthly precipitation data that were obtained from the Scenarios Network for Alaska and Arctic Planning (SNAP, 2014). The original climate data were derived from the University of East Anglia Climatic Research Unit gridded high-resolution (0.5°×0.5°) global climate dataset (1901 to 2009) (CRU TS v. 3.10.01; New and others, 1999, 2000; Harris and others, 2014). The SNAP team extracted data for the State of Alaska and western Canada from the global dataset, and these files were bias corrected and downscaled via the delta method using the 1961–1990 Parameter-elevation Relationships on Independent Slopes Model (PRISM; PRISM Climate Group, 2004). These data were averaged and processed into pixel-specific basin averages using the continuous parameterization technique of Verdin and Worstell (2008). The discharge estimates were developed for the entire Alaska land mass and transferred onto the EDNA-derived stream network.

Alaska is not a self-contained drainage system, as portions of some watersheds lie within Canada. The EDNA database does not extend into Canada; therefore, the Canadian portion of the drainage basin and the associated flow estimates were developed using the National Aeronautics and Space Administration Shuttle Radar Topographic Mission data (NASA-SRTM; Jarvis and others, 2008). Discharge derived from these basins was calculated and propagated into the Canadian flow network through the EDNA-derived drainage network in Alaska. This report accounts for the discharge coming from Canada for basins with a greater-than-10-$km^2$ drainage threshold.

The National Hydrography Dataset (NHD, at a scale of 1:63,360; U.S. Geological Survey, 2014a) was used to estimate the number and area of lakes in Alaska. The NHD data were compiled to meet the National Map Accuracy Standards. Within the NHD water body geodatabase attributes, vectors classified as reservoirs, lakes, or ponds were extracted to represent surface water extents in each of the study areas.

Discharge, watershed area, and lake area were summarized by 4-digit hydrologic regions using the U.S. Geological Survey (USGS) Hydrologic Unit Codes (HUCs; Seaber and others, 1987). There are six 4-digit hydrologic regions covering the State of Alaska (fig. 8.1).

## 8.3.3. Coastal Export of Carbon From Riverine Systems

Alkalinity, temperature, and pH measurements for rivers in Alaska were obtained from the USGS's National Water Information Service (NWIS; U.S. Geological Survey, 2014b),

the U.S. Environmental Protection Agency's Storage and Retrieval System (STORET; U.S. Environmental Protection Agency, 2014), and the Pebble Partnership's baseline water-quality datasets for the Bristol Bay and Cook Inlet drainages (Pebble Partnership, 2011a,b). We converted the various alkalinity measurements (alkalinity, bicarbonate, carbonate, and acid neutralizing capacity) to "alkalinity as calcium carbonate." Organic acids are a major contributor to noncarbonate alkalinity at low pH levels (Driscoll and others, 1989). We did not have enough organic carbon data to pair with our alkalinity data to directly estimate organic acid contribution to alkalinity, but we did remove alkalinity values that had an associated pH of less than 5.6 (Driscoll and others, 1989). Only sites with paired daily alkalinity, temperature, and pH data for 1970 to 2013 were used in this assessment. These 7,563 data points were representative of 1,301 individual sites on rivers throughout Alaska (fig. 8.3*A*).

Estimated dissolved DIC, composed of $CO_2$, bicarbonate, and carbonate, was computed using the speciation model of PHREEQC (Parkhurst and Appelo, 1999; Charlton and others, 2014). Required input variables were water temperature, pH, and alkalinity concentrations. We removed any DIC estimates that fell outside of the interval (Q1–IQR, Q3+IQR), where IQR is the interquartile range and Q1 and Q3 are the first and third quartiles, respectively. This resulted in the removal of 18 data points, so that our final DIC concentration dataset had 7,545 data points from 1,296 sites.

Dissolved organic carbon (DOC) and total organic carbon (TOC) values for rivers in Alaska were obtained from NWIS (U.S. Geological Survey, 2014b), the Pebble Partnership (2011a,b), and from various existing datasets in the Southwest (Daniel E. Schindler and Gordon Holtgrieve, University of Washington, unpub. data, October 23, 2013), Northwest (Larouche and others, 2012), and North Slope regions (Josh Koch, USGS, Anchorage, Alaska, unpub. data, November 5, 2013). We compiled a total of 1,679 DOC samples and 623 TOC samples. To use the more extensive DOC concentration dataset in our TOC flux estimates, we built a simple-linear-regression (SLR) model between paired TOC and DOC collected at the same site on the same day. We used the results of the SLR ($R^2 = 0.88$, $y = 0.25 + 1.00481x$, where $R^2$ is the coefficient of determination, $x$ is the DOC concentration, and $y$ is the TOC concentration) to predict TOC from the extensive DOC dataset. This process resulted in a TOC dataset with 2,574 samples from 519 sites. We removed any samples that fell outside of the interquartile range as described above. This resulted in the removal of 14 data points, so that our final TOC concentration dataset had 2,560 data points from 515 sites.

Carbon fluxes for coastal watersheds in Alaska were estimated in three different ways, depending on the amount of data available for each particular watershed. For coastal watersheds that contained USGS gaging stations with robust DIC and TOC concentration datasets and 3 years or more of daily discharge, carbon fluxes were estimated using the USGS Load Estimator program (LOADEST; Runkel and others, 2004). LOADEST is a multiple-regression adjusted maximum likelihood estimation model that uses measured DIC or TOC concentration values to calibrate a regression between constituent load, streamflow, seasonality, and time. The model requires at least 13 paired concentration and daily discharge values. Daily streamflow values were downloaded from NWIS. The LOADEST model uses the Akaike (1981) Information Criterion (AIC) to select the best combination of coefficients at each streamgage station from the full model, which is based on the equation:

$$\ln Flux = a_0 + a_1 \ln Q + a_2 \ln Q^2 + a_3 \sin(2\pi dtime) + a_4 \cos(2\pi dtime) + a_5 dtime + a_6 dtime^2 + \varepsilon \quad (8.2)$$

where

$\ln Flux$ is the natural log of the constituent flux, in kilograms per day (kg/d),

$Q$ is the discharge, in $m^3/s$,

$dtime$ is time, in decimal years,

$a_0, a_1, \ldots a_6$ are regression coefficients, and

$\varepsilon$ is an independent and normally distributed error.

The input data were log-transformed to avoid bias and centered to avoid multicollinearity. The model produces a flux estimate (in kg/d) with standard error values, which were used to create a distribution of LOADEST modeled fluxes for these watersheds.

For coastal watersheds that had 3 years or more of daily discharge but did not have sufficient concentration records for use in the LOADEST model, we multiplied carbon concentration by discharge to obtain a flux using the following equation:

$$Flux = C \times Q \quad (8.3)$$

where

$Flux$ is the constituent flux, in kg/d,

$C$ is carbon concentration of surface water at the site, in milligrams per liter (mg/L), and

$Q$ is discharge, in $m^3/s$.

A specified range of discharge and concentration values were used in equation 8.3 for each watershed. The distribution of empirical streamflow for each watershed was based on the standard deviation (s.d.) of recorded flows for that site. The distribution of carbon concentrations was based on all available carbon concentrations within that regional HUC. If the coastal watershed lay within the boundaries of the Southeast region, then the concentration distribution for that watershed was drawn from all concentration values within that region. In the Southeast region, 226 DIC values and 45 TOC measurements were used to create the concentration distributions.

***A.*** **Riverine lateral carbon fluxes to coastal waters**

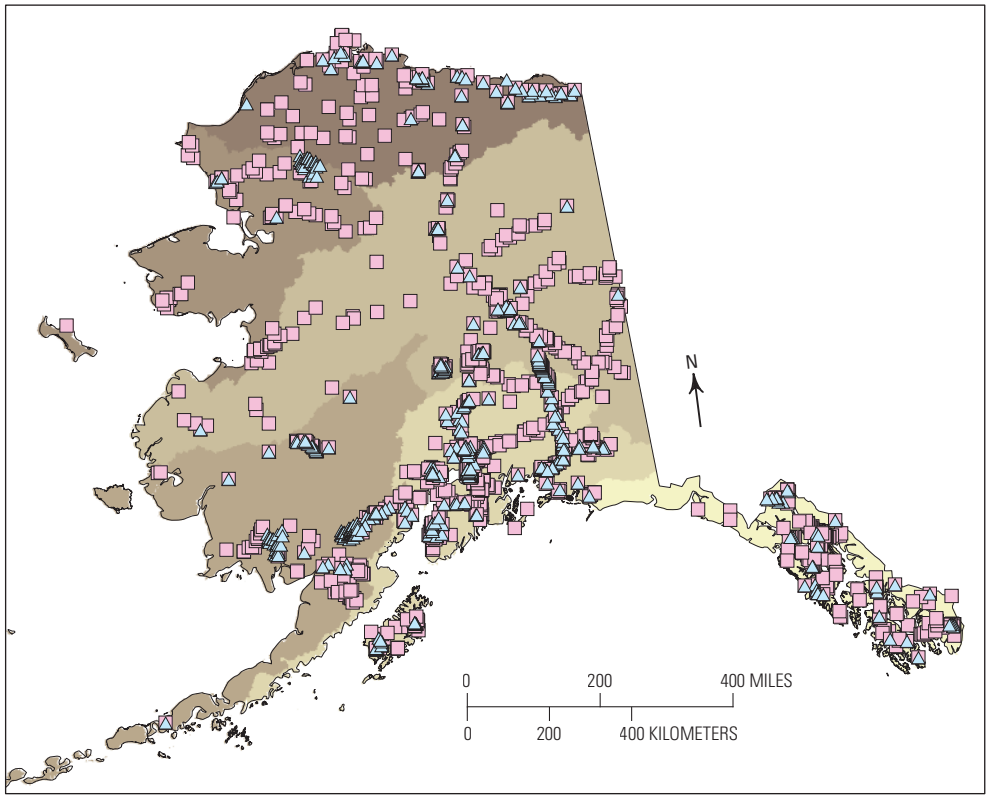


**EXPLANATION**

**Carbon yield, in grams of carbon per square meter per year**

- 0 to 4
- >4 to 8.7
- >8.7 to 9.0
- >9.0 to 10.5
- >10.5 to 16.9
- >16.9 to 36.7

**Carbon sample used for analysis**

- △ Total organic carbon
- □ Dissolved inorganic carbon

***B.*** **Riverine carbon dioxide emissions**

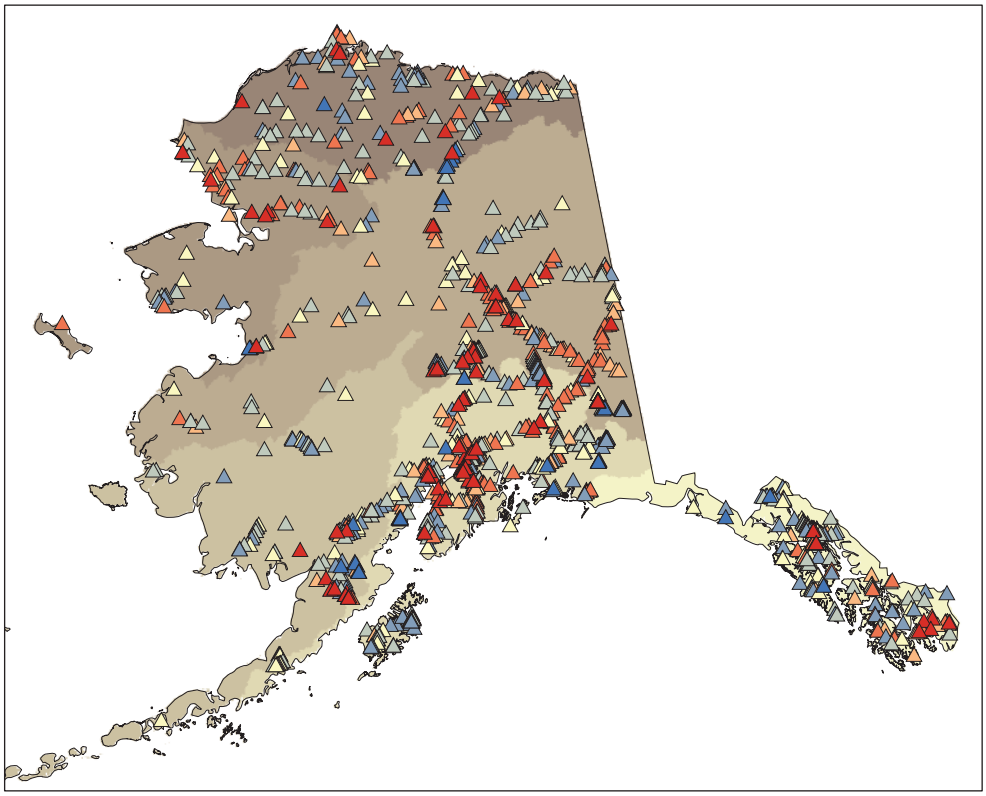

**Carbon yield, in grams of carbon per square meter per year**

- 0 to 4
- >4 to 5.2
- >5.2 to 8.0
- >8.0 to 11.2
- >11.2 to 21.2
- >21.2 to 36.0

**Partial pressure of carbon dioxide, in microatmospheres**

- 0 to 400
- >400 to 1,000
- >1,000 to 2,000
- >2,000 to 3,000
- >3,000 to 4,000
- >4000 to 10,000
- >10,000

**Figure 8.3.** Estimated relative magnitude of carbon yields. *A*, Coastal carbon transport by rivers. *B*, Carbon dioxide ($CO_2$) emissions from rivers. *C*, $CO_2$ emissions from lakes. *D*, Carbon burial rates in lakes. *B* and *C* also indicate the estimated relative magnitude of the partial pressure of $CO_2$ ($pCO_2$) concentrations at the sampling locations.

***C.*** **Lacustrine carbon dioxide emissions**

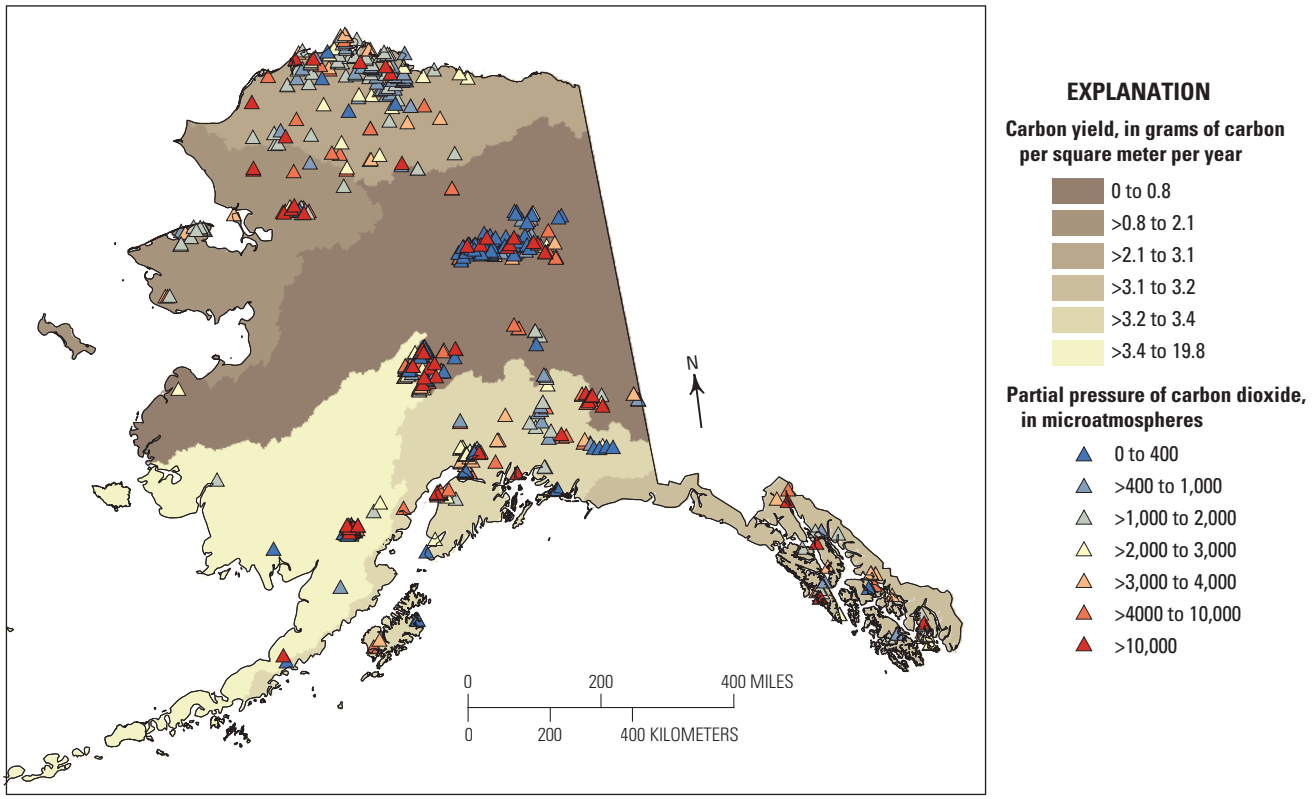


***D.*** **Lacustrine organic carbon burial**

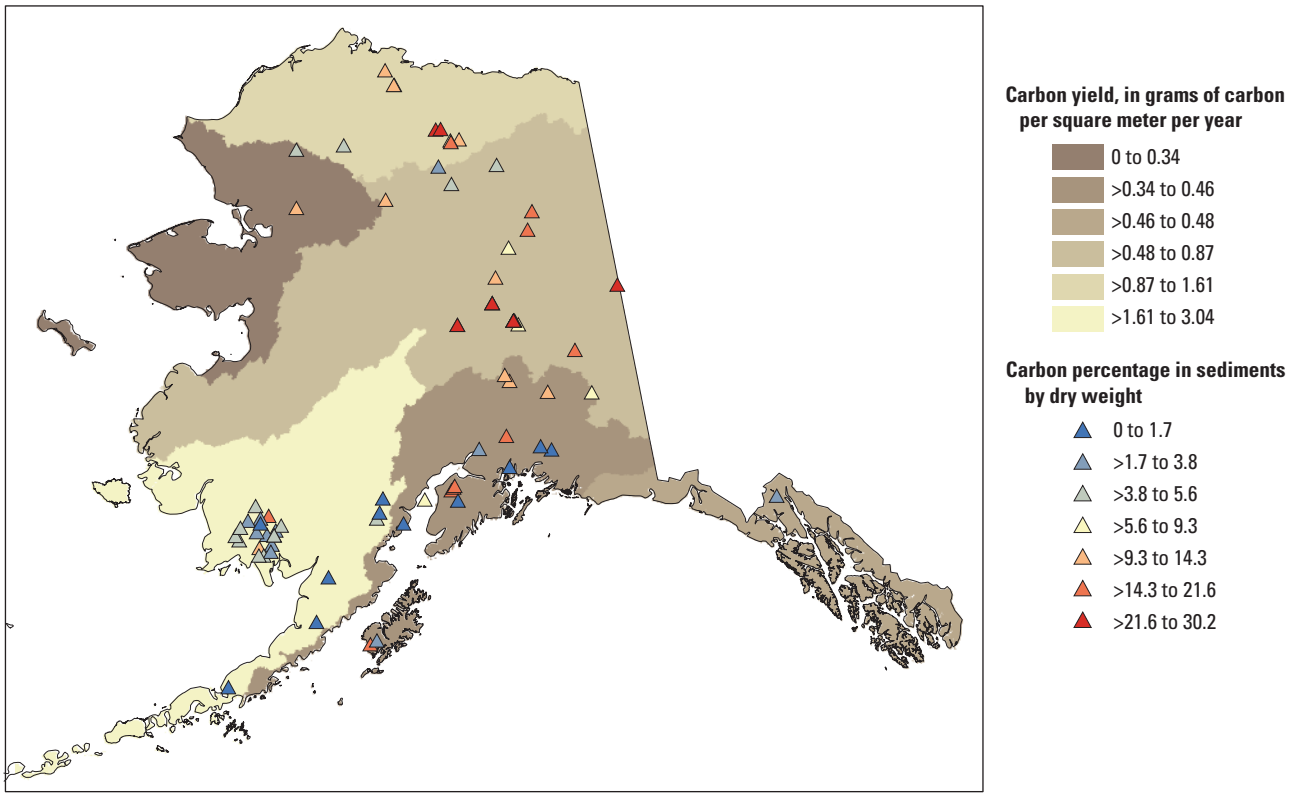


**Figure 8.3.** Estimated relative magnitude of carbon yields. *A*, Coastal carbon transport by rivers. *B*, Carbon dioxide ($CO_2$) emissions from rivers. *C*, $CO_2$ emissions from lakes. *D*, Carbon burial rates in lakes. *B* and *C* also indicate the estimated relative magnitude of the partial pressure of $CO_2$ ($pCO_2$) concentrations at the sampling locations.—Continued

If empirical carbon concentration and streamflow data were not available for a watershed, the distribution of carbon concentrations was established as described in the previous paragraph. To generate a distribution of discharge values for each watershed, we developed prediction intervals of discharge estimated using EDNA (see section 8.3.2) using the predict function in R (R Development Core Team, 2008). The predict function was based on the output from a simple linear model that describes estimated EDNA discharge values by empirical NWIS discharge values.

We used the distribution of LOADEST fluxes, concentrations, and discharge values as described in the previous three paragraphs in a Monte Carlo approach with 10,000 iterations to estimate total flux estimates for the approximately 6,000 coastal watersheds draining Alaska. The DIC and TOC fluxes were summed for each watershed, and the fluxes from all the watersheds within a region were summed, so that each of the six regions had 10,000 possible total carbon flux estimates. The median flux with 5th and 95th percentiles from that range of values are presented in table 8.1. Yields were calculated by dividing the total carbon flux by HUC area. The percent of the total area of the State of Alaska that was represented by LOADEST modeled fluxes (equation 8.2) was 75 percent for DIC and 65 percent for TOC, and the carbon fluxes for the remainder of the land surface area were estimated using equation 8.3.

The contribution of the Canadian drainage area to the total Alaskan coastal carbon flux estimates is also presented in table 8.1. The Yukon River, along with several smaller rivers in the Southeast and South-Central regions that drain into the Gulf of Alaska, has headwaters in Canada. We used equation 8.2 to estimate Yukon River carbon sourced in Canada with discharge and DIC and TOC concentration data (1990–2005) from a streamgage just inside the border of Alaska, the Yukon River at Eagle (NWIS station ID=15356000). We used equation 8.3 to estimate carbon fluxes from Canada for rivers in the Southeast and South-Central regions, including the Alsek, Stikine, and Taku Rivers, with EDNA-derived discharge values and carbon concentration values from Environment and Climate Change Canada (2014).

**Table 8.1.** Estimated coastal carbon exports and yields from riverine systems in Alaska.

[Sites are locations for which dissolved inorganic carbon (DIC) or total organic carbon (TOC) concentration data were available. Values are estimates of the median with 5th and 95th percentile estimates in parentheses. Total exports and total yields were calculated by summing dissolved inorganic carbon (DIC) and total organic carbon (TOC). $km^2$, square kilometer; DIC, dissolved inorganic carbon; TOC, total organic carbon; $km^3/yr$, cubic kilometer per year; TgC/yr, teragram of carbon per year; $gC/m^2/yr$, gram of carbon per square meter per year]

| Hydrologic region | Area of hydrologic region ($km^2$) | Number of sites with concentration data | | Estimated total discharge ($km^3/yr$) | Estimated total carbon export (TgC/yr) | Estimated total carbon yield ($gC/m^2/yr$) | Estimated carbon export as DIC (percent) |
|---|---|---|---|---|---|---|---|
| | | DIC | TOC | | | | |
| Southeast | 104,000 | 226 | 45 | 356 (297, 569) | 3.8 (3.4, 5.3)[a] | 36.7 (32.4, 50.7) | 67.2 |
| South-Central | 207,000 | 454 | 185 | 220 (156, 514) | 3.5 (3.1, 5.0)[b] | 17.0 (15.1, 24.0) | 73.5 |
| Southwest | 291,000 | 169 | 130 | 174 (142, 260) | 2.7 (2.2, 3.4) | 9.2 (7.7, 11.6) | 78.4 |
| Yukon | 526,000 | 264 | 73 | 144 (35, 685) | 5.5 (5.4, 5.7)[c] | 10.5 (10.2, 10.8) | 67.1 |
| Northwest | 178,000 | 76 | 31 | 69 (52, 176) | 1.5 (1.3, 3.4) | 8.7 (7.2, 19.0) | 76.7 |
| North Slope | 204,000 | 107 | 51 | 53 (44, 132) | 1.3 (0.9, 2.3) | 6.1 (4.3, 11.5) | 62.3 |
| **Total or mean** | **1,510,000** | **1,296** | **515** | **1,015 (725, 2,237)** | **18.3 (16.3, 25.0)** | **12.2 (10.8, 16.6)** | **69.8** |

[a]Includes estimated sum lateral flux from transboundary Canadian rivers into the Southeast region of 0.13 (0.1, 0.17) TgC/yr.

[b]Includes estimated sum lateral flux from transboundary Canadian rivers into the South-Central region of 2.7 (2.1, 3.4) TgC/yr.

[c]Includes estimated sum lateral flux from transboundary Canadian rivers into the Yukon region of 1.7 (1.6, 1.8) TgC/yr.

## 8.3.4. Carbon Dioxide Flux From Riverine Systems

Three variables were required to estimate the $CO_2$ gas fluxes from aquatic systems: (1) the concentration of dissolved $CO_2$, (2) the gas transfer velocity, and (3) the surface area of the water body. The $CO_2$ emission from rivers (and lakes, see section 8.3.5) across Alaska was modeled according to established methods (Butman and Raymond, 2011; Zhu and Reed, 2012, 2014) and as outlined in equation 8.4:

$$CO_2\ flux = (CO_{2\text{-}water} - CO_{2\text{-}air}) \times kCO_2 \times SA \qquad (8.4)$$

where

$CO_2\ flux$ is the total net emission of $CO_2$ from rivers of Alaska, in teragrams of carbon per year (TgC/yr),

$CO_{2\text{-}water}$ is the $CO_2$ concentration of the water, in moles per liter (mol/L),

$CO_{2\text{-}air}$ is the $CO_2$ concentration in the atmosphere, in mol/L,

$kCO_2$ is the river or lake gas transfer velocity of $CO_2$ across the air-water interface, in meters per day (m/d), and

$SA$ is the river or lake surface area, in square meters ($m^2$).

The total flux was estimated by summing all of the mean annual fluxes for a stream order (Strahler, 1952) within a hydrologic region.

The median dissolved $CO_2$ concentrations ($CO_{2\text{-}water}$) were estimated from stream and river alkalinity data available from the same three data sources listed in section 8.3.3. All alkalinity measurements were converted to dissolved $CO_2$ using the CO2SYS program (Van Heuven and others, 2011). Daily measurements of pH paired with temperature and alkalinity measurements from the late 1960s through 2013 were used to estimate dissolved $CO_2$. Similar to the methods described in section 8.3.3, alkalinity data with an associated pH of less than 5.6 were removed to reduce the effect of organic acids on alkalinity (Driscoll and others, 1989). A total of 9,466 daily chemical measurements from 1,469 sampling locations was used (fig. 8.3*B*). For equation 8.4, current atmospheric partial pressure of carbon dioxide ($pCO_2$) was assumed to be 390 microatmospheres (µatm) for all of the hydrologic regions across Alaska.

The gas transfer velocity ($kCO_2$) was modeled based on a meta-analysis of measurements of gas exchange and the gas transfer velocity made by direct tracer injections across small- to mid-sized river systems in the United States (Melching and Flores, 1999; Raymond and others, 2012). The variation in gas transfer velocities within rivers was a function of turbulence at the air-water interface (Zappa and others, 2007). Physical parameters of stream slope and water velocity were used to predict gas transfer velocity:

$$kCO_{2\text{–}river} = S \times V \times 2{,}841.6 + 2.03 \qquad (8.5)$$

where

$kCO_{2\text{–}river}$ is the gas transfer velocity of $CO_2$ (in m/d) normalized to the Schmidt number (a dimensionless ratio that approximates the relationship between the viscosity and gas diffusivity across a boundary layer) for $CO_2$ at ambient water temperature and standard atmospheric pressure (Wanninkhof, 1992; Raymond and others, 2012),

$S$ is the average slope of a stream reach, and

$V$ is the average velocity of water, in m/d.

A total of 563 independent gas tracer injection measurements was included in the development of this equation.

A total of 32,672 discharge measurements was used to derive hydraulic geometry coefficients specific to each hydrologic region. Hydraulic geometry of stream reaches showed remarkable consistency to approximate channel width within and across watersheds (Leopold and Maddock, 1953; Park, 1977). All scaling relationships to estimate width derived by the calculation of hydraulic geometry coefficients were statistically significant (p-value$<$0.001) with coefficients ranging from 0.46 in the Southeast region to 0.57 in the Southwest region. $R^2$ values for the nonlinear regression between width and stream discharge ranged from 0.90 to 0.96. Modeled average annual discharge (see section 8.3.2) was used to estimate average channel width and velocity using the hydraulic geometry coefficients specific to each hydrologic region. Both stream velocity and slope estimates were normalized by total length and aggregated to hydrologic regions by stream order. Average slope and velocity were then calculated by stream order to estimate the gas transfer velocity of $CO_2$ according to equation 8.5.

River surface area ($SA$) was calculated based on the same hydraulic geometry coefficients discussed above for width within each hydrologic region. Average discharge was used to then calculate an average width for each stream order within a hydrologic region. The total stream length was then calculated for each stream order within a hydrologic region. Stream and river surface area was then calculated as the product of the average width and total length of streams by stream order.

Error propagation and uncertainty analyses were performed for each component of equation 8.4. To estimate error, we utilized a bootstrapping technique as outlined in Efron and Tibshirani (1994) and Butman and Raymond (2011). Bootstrap with replacement was run for 1,000 iterations to calculate 95 percent confidence intervals for the $pCO_2$ values for each stream order within a hydrologic region. Similarly, bootstrap with replacement was used to estimate confidence intervals associated with the hydraulic geometry coefficients derived from the measurements of stream width and velocity, which were subsequently used to estimate both the river surface area and gas transfer velocity. Overall bias associated with estimates of $pCO_2$ remained low and had a negligible effect on the error associated with the use of the median value for each stream order. Similarly, the effect of bootstrapping the hydraulic geometry coefficients produced minimal bias.

A Monte Carlo simulation was performed for each stream order estimate of the total flux (in TgC/yr) from river surfaces (equation 8.4). The confidences derived from the bootstrapping procedure were used to bound the Monte Carlo simulation for each parameter of equation 8.4. The total flux calculation was replicated 1,000 times. Gas transfer velocities were not permitted to exceed 30 m/d. This selection criterion only affected first through third stream orders in the Southeast and South-Central regions. This constraint was placed because of the lack of measurements above that value presented in Raymond and others (2012), and there is a lack of evidence in the literature that small streams can exceed this threshold.

All estimates for the total carbon flux within each hydrologic unit were presented with the 5th and 95th percentiles derived from the Monte Carlo simulation. This approach is considered conservative as it allowed for the same probability for all combinations of each parameter in the total flux equation to be selected for each stream order and may have overestimated the error associated with the river $CO_2$ emission. In general, this conservative approach biased the range of estimates high owing to a slight skew in the distribution of $pCO_2$ values within a stream order and hydrologic region. But by using median values and bootstrapped 5th and 95th percentiles, this skew is minimized. All estimates derived from the Monte Carlo simulation were adjusted to account for monthly temperatures below freezing under the assumption that river $CO_2$ emission did not occur when monthly temperatures averaged below 0 degrees Celsius (°C). Average monthly temperatures were derived from the WorldClim 1-km monthly averages spanning from 1950 to 2000 (Hijmans and others, 2004). Each stream segment was attributed with a proportion of the year as frozen. This adjustment reduced the efflux for the Southeast region by 32 percent, South-Central region by 50 percent, Southwest region by 54 percent, Yukon region by 59 percent, Northwest region by 62 percent, and North Slope region by 69 percent.

## 8.3.5. Carbon Dioxide Flux From Lacustrine Systems

Water-chemistry data used to estimate lake $CO_2$ emissions from Alaska were obtained from NWIS (U.S. Geological Survey, 2014b), STORET (U.S. Environmental Protection Agency, 2014), the Pebble Partnership (2011a,b), the U.S. National Park Service Shallow Lake Monitoring Program (Larsen and Kristenson, 2012), and the dataset from studies of lakes at Yukon Flats, Alaska (Halm and Guldager, 2013; Halm and Griffith, 2014). A total of 891 locations and 1,329 measurements with daily lake chemistry data suitable for $CO_2$ emission estimates collected between 1949 and 2011 (fig. 8.3*C*) were used in this study.

The estimated $CO_2$ emission from lakes was also calculated using the general equation 8.4. Dissolved $CO_2$ values were also calculated using the CO2SYS program (Van Heuven and others, 2011). We did not have enough organic carbon data to pair with our alkalinity data to directly measure organic acid contribution to alkalinity. In general, noncarbonate alkalinity will introduce a bias resulting in higher alkalinity generating a higher calculated $pCO_2$; however, a recent estimate of bias for the evasion of $CO_2$ from lakes in the conterminous United States suggests that this will alter flux measurements by no more than 2 to 5 percent (McDonald and others, 2013).

All lakes within the high-resolution NHD were attributed with average summer wind speed ($U_{10}$), median $pCO_2$, and the annual ice-free fraction needed to calculate the vertical efflux of carbon. This method differs from those of McDonald and others (2013) in that, for Alaska, a single flux is calculated for each specific lake and then aggregated into regional estimates. McDonald others (2013) summed lake area only by region, then used average ecoregional wind speed and carbon concentrations to calculate fluxes.

The gas transfer velocity for lakes ($kCO_{2-lake}$) was calculated as a function of wind speed (Cole and Caraco, 1998; Cole and others, 2007):

$$kCO_{2-lake} = 2.07 + 0.215 \times U_{10}^{1.7} \quad (8.6)$$

where

$kCO_{2-lake}$ is a gas transfer coefficient normalized to ambient water temperature and atmospheric pressure (STP), in m/d, and

$U_{10}$ is the surface wind speed above the lake surface, in m/d.

The estimated mean summer (June to September) wind speeds for each hydrologic region were determined from the National Aeronautics and Space Administration (NASA; 2014) surface meteorology and solar energy data. Each lake within the NHD was assigned a $CO_2$-specific transfer coefficient for lake surface efflux.

Many of the parameters involved in these calculations violated normality assumptions; therefore, nonparametric

confidence intervals (95 percent) were determined on 10,000 ordinary bootstrap replicates. Bootstrapped nonparametric confidence intervals for median $pCO_2$ values were calculated in R using the bias corrected and accelerated methods of Efron and Tibshirani (1994) in each distribution of values by hydrologic region. Median values were chosen owing to the highly skewed distributions of concentration data. Bootstrapped confidence intervals for water temperature were similarly calculated. In general, water temperature was normally distributed about the mean value allowing normal confidence intervals to be used. Each lake within a region was assumed to have a range of potential dissolved $CO_2$ within the calculated nonparametric confidence intervals. The total flux by region was calculated holding the average wind speed for a lake constant. In the case of the total flux from Alaska, the 5th and 95th percentiles were assumed to be additive (uncertainty was not propagated) because potential errors in the regional estimates were likely to be systematic. Similar to the methods for river $CO_2$ emission, each lake within a region was attributed with a scalar representing the proportion of the year below freezing, when flux was assumed to equal zero. This scalar was applied to each lake and had the same reducing effect as for river $CO_2$ emission. This approach was conservative because $CO_2$ produced and stored under ice is commonly released rapidly when the ice melts (Anderson and others, 1999). Final estimates represent total fluxes for each hydrologic region, with 5th and 95th percentiles.

## 8.3.6. Carbon Burial in Lacustrine Systems

Carbon burial in lakes, which is a function of sedimentation rates, bulk density of the sediment, sediment carbon concentrations, and lake area (Mulholland and Elwood, 1982; Dean and Gorham, 1998), was estimated as:

$$C_{burial} = SA_{WB} \times SedRt \times C_{conc} \times 10^{-12} \quad (8.7)$$

where

$C_{burial}$ is the carbon burial rate, in TgC/yr,

$SA_{WB}$ is the surface area of the water body, in $m^2$,

$SedRt$ is the sedimentation rate, in grams of carbon per square meter per year ($gC/m^2/yr$),

$C_{conc}$ is the concentration of carbon in sediments (percent carbon by dry weight of sediment divided by 100), and

$10^{-12}$ is a conversion factor to convert from grams to teragrams.

Water body surface areas were derived from the high-resolution NHD and included lakes, ponds, and reservoirs. We did not differentiate between lakes and reservoirs in this report. Data on sedimentation rates and lake sediment carbon concentrations were derived from previously collected and dated sediment cores from 70 Alaskan lakes; these data were obtained from published and unpublished sources (table 8.2; fig. 8.3*D*). The cores were dated using $^{210}Pb$ and $^{137}Cs$ isotope techniques, as well as $^{14}C$ dating of terrestrial plants deposited in near-surface layers. Sedimentation results pertain to the most recent 100 years of sediment accumulation, which typically corresponds to the top 5 to 15 centimeters (cm) of sediment, depending on sedimentation rates. For $^{14}C$-dated cores, sedimentation rates were interpolated based on linear sedimentation rates from the most recent $^{14}C$ date to the top of the core, which we assumed represents the year of collection.

Data from the cores were used to build geostatistical models for sedimentation rates and sediment carbon concentrations using stepwise multiple linear regression (MLR); these predictive equations were applied statewide. Potential explanatory variables included lake area and lake elevation from the NHD, mean annual precipitation and temperature from SNAP, vegetation characteristics from the National Land Cover Database (NLCD) 2006 (Fry and others, 2011), permafrost and bog extent from chapters 3 and 7 of this report, and soil organic carbon in the top 152 cm of soil from the state soil geographic database (STATSGO; U.S. Department of Agriculture, Natural Resource Conservation Service, 2014). Each of these parameters was calculated for the 12-digit HUC that intersected each water body. In the MLR, the independent variable that explained the most variance in the dependent variable entered the model first. The variances explained by the remaining independent variables were recalculated, and the variable that explained the next greatest amount of variance entered the model next. This iterative process was repeated until the minimum AIC was obtained (Akaike, 1981). Multicollinearity among explanatory variables was evaluated using the variance inflation factor ($1/(1–R^2)$; Hair and others, 2006) with a threshold for exclusion of 2.0. Uncertainty in model predications was evaluated by using a Monte Carlo approach in which the coefficients for model parameters were allowed to vary randomly within their 5th and 95th percentiles; this procedure was repeated for 1,000 iterations, yielding 1,000 estimates of sedimentation rate and sediment carbon concentration for each water body in the Alaska NHD. Results are summarized for each of the six hydrologic regions in Alaska.

## 8.3.7. Limitations and Uncertainties

Methods used to calculate river dissolved carbon fluxes to the coast had some limitations. For 25 to 35 percent of the land surface area, carbon flux was calculated simply as flow multiplied by concentration (equation 8.3), which does not allow for variability in seasonal discharge of carbon concentrations (Runkel and others, 2004). Additionally, the concentration data used in the coastal flux estimates had relatively good spatial coverage, and watersheds with DIC or TOC concentrations represented over 50 percent of the

**Table 8.2.** Site information and data sources used to develop multiple-linear-regression models for estimation of carbon burial in Alaskan water bodies.

[Data included sediment carbon concentrations, sediment accumulation rates, and dry bulk density. Coordinates are in decimal degrees, NAD 83; HUC; hydrologic unit code; 1901, Southeast hydrologic region; 1902; South-Central hydrologic region; 1903, Southwest hydrologic region; 1904, Yukon hydrologic region; 1905, Northwest hydrologic region; 1906, North Slope hydrologic region]

| 4-digit HUC | Site name | Latitude | Longitude | References and data sources |
|---|---|---|---|---|
| 1901 | Chilkat Lake | 59.33 | –135.90 | Barto (2004) |
| 1902 | Long Lake | 62.55 | –143.40 | N. Bigelow, University of Alaska-Fairbanks, unpub. data (2014) |
| 1902 | Hickerson Lake | 59.93 | –152.92 | Cohn (2009) |
| 1902 | Frazer Lake | 57.26 | –154.14 | B. Finney, Idaho State University, unpub. data (2014) |
| 1902 | Coghill Lake | 61.09 | –147.82 | B. Finney, Idaho State University, unpub. data (2014) |
| 1902 | Phalarope Lake | 57.18 | –154.41 | Jones, Peteet, and others (2009) |
| 1902 | Rock Lake | 60.65 | –150.64 | Lynch and others (2002) |
| 1902 | Arrow Lake | 60.75 | –150.49 | Lynch and others (2002) |
| 1902 | Portage Lake | 60.72 | –150.53 | Lynch and others (2002); Hinzman and others (2005) |
| 1902 | Greyling Lake | 61.38 | –145.74 | McKay and Kaufman (2009) |
| 1902 | Hallet Lake | 61.49 | –146.24 | McKay and Kaufman (2009) |
| 1902 | Skilak Lake | 60.42 | –150.37 | Naidu and others (1999) |
| 1902 | Packer Lake | 60.47 | –151.92 | Rogers and others (2013) |
| 1902 | Swampbuggy Lake | 63.05 | –147.42 | Rohr (2001) |
| 1902 | Nutella Lake | 63.20 | –147.63 | Rohr (2001) |
| 1902 | Canyon Lake | 62.70 | –145.57 | Shimer (2009) |
| 1902 | Kepler Lake | 61.55 | –149.21 | Yu and others (2008) |
| 1902 | Hundred Mile Lake | 61.81 | –147.85 | Yu and others (2008) |
| 1903 | Little Swift Lake | 60.22 | –159.77 | Axford and Kaufman (2004) |
| 1903 | Ongoke Lake | 59.27 | –159.43 | Chipman and others (2009) |
| 1903 | Kontrashabuna Lake | 60.19 | –154.03 | Cohn (2009) |
| 1903 | Portage Lake | 60.50 | –153.86 | Cohn (2009) |
| 1903 | Lower Ugashik Lake | 57.66 | –156.73 | B. Finney, Idaho State University, unpub. data (2014) |
| 1903 | Lone Spruce Pond | 60.01 | –159.15 | Kaufman and others (2012) |
| 1903 | Aleknagik Lake | 59.36 | –158.89 | Rogers and others (2013) |
| 1903 | Amanka Lake | 59.10 | –159.22 | Rogers and others (2013) |
| 1903 | Bear Lake | 56.02 | –160.25 | Rogers and others (2013) |
| 1903 | Beverly Lake | 59.68 | –158.77 | Rogers and others (2013) |
| 1903 | Gechiak Lake | 59.39 | –160.37 | Rogers and others (2013) |
| 1903 | Goodnews Lake | 59.49 | –160.56 | Rogers and others (2013) |
| 1903 | Grant Lake | 59.81 | –158.53 | Rogers and others (2013) |
| 1903 | High Lake | 59.94 | –159.50 | Rogers and others (2013) |
| 1903 | Kagati Lake | 59.87 | –160.06 | Rogers and others (2013) |
| 1903 | Little Togiak Lake | 59.58 | –159.15 | Rogers and others (2013) |
| 1903 | Nagugun Lake | 59.69 | –160.39 | Rogers and others (2013) |
| 1903 | Naknek Lake | 58.69 | –156.28 | Rogers and others (2013) |
| 1903 | Nerka Lake | 59.58 | –158.83 | Rogers and others (2013) |
| 1903 | Nunavaugaluk Lake | 59.20 | –158.91 | Rogers and others (2013) |
| 1903 | Tazmina Lake | 60.05 | –154.15 | Rogers and others (2013) |
| 1903 | Togiak Lake | 59.61 | –159.62 | Rogers and others (2013) |
| 1903 | Ualik Lake | 59.09 | –159.44 | Rogers and others (2013) |
| 1903 | Upper Togiak Lake | 59.83 | –159.48 | Rogers and others (2013) |

**Table 8.2.** Site information and data sources used to develop multiple-linear-regression models for estimation of carbon burial in Alaskan water bodies.—Continued

[Data included sediment carbon concentrations, sediment accumulation rates, and dry bulk density. Coordinates are in decimal degrees, NAD 83; HUC; hydrologic unit code; 1901, Southeast hydrologic region; 1902; South-Central hydrologic region; 1903, Southwest hydrologic region; 1904, Yukon hydrologic region; 1905, Northwest hydrologic region; 1906, North Slope hydrologic region]

| 4-digit HUC | Site name | Latitude | Longitude | References and data sources |
|---|---|---|---|---|
| 1904 | Birch Lake | 64.31 | –146.66 | Abbott and others (2000) |
| 1904 | Tangled Up Lake | 67.67 | –149.72 | Anderson and others (2001) |
| 1904 | Track Lake | 66.86 | –145.17 | D. Anderson, U.S. Geological Survey, unpub. data (2014) |
| 1904 | Greenpepper Lake | 66.09 | –146.73 | D. Anderson, U.S. Geological Survey, unpub. data (2014) |
| 1904 | Twelve-Mile Lake | 66.45 | –145.55 | D. Anderson, U.S. Geological Survey, unpub. data (2014) |
| 1904 | Six Mile Lake | 64.87 | –141.12 | N. Bigelow, University of Alaska-Fairbanks, unpub. data (2014) |
| 1904 | Little Harding Lake | 64.41 | –146.90 | Brady (2013) |
| 1904 | Jan Lake | 63.56 | –143.92 | Carlson and Finney (2004) |
| 1904 | Keche Lake | 68.02 | –146.93 | Chipman and others (2012) |
| 1904 | Takahula Lake | 67.35 | –153.67 | Clegg and Hu (2010) |
| 1904 | Harding Lake | 64.42 | –146.85 | Finkenbinder and others (2014) |
| 1904 | Dune Lake | 64.42 | –149.90 | Finney and others (2012) |
| 1904 | Oops Lake | 65.44 | –147.63 | Finney, University of Idaho, unpub. data (2014) |
| 1904 | Ace Lake | 64.86 | –147.94 | B. Gaglioti, University of Alaska-Fairbanks, unpub. data (2014) |
| 1904 | Deuce Lake | 64.86 | –147.94 | Lynch and others (2002) |
| 1905 | Burial Lake | 68.43 | –159.17 | Abbott and others (2010) |
| 1905 | Lake Wolverine | 67.09 | –158.92 | Mann and others (2002) |
| 1906 | Meli Lake | 68.68 | –149.08 | Anderson and others (2001) |
| 1906 | Blue Lake | 68.09 | –150.47 | Bird and others (2009) |
| 1906 | Lake Helen | 70.36 | –153.68 | B. Gaglioti, University of Alaska-Fairbanks, unpub. data (2014) |
| 1906 | Nikivlik Lake | 68.59 | –156.25 | B. Gaglioti, University of Alaska-Fairbanks, unpub. data (2014) |
| 1906 | Dimple Lake | 68.94 | –150.50 | Johnson and others (2011) |
| 1906 | NE-14 | 68.67 | –149.63 | Johnson and others (2011) |
| 1906 | Perch Lake | 68.95 | –150.20 | Johnson and others (2011) |
| 1906 | Toolik Lake | 68.63 | –149.61 | Johnson and others (2011) |

total regional area. There were some gaps, however, and the watersheds that contained DIC concentration data only represented 16 percent of the total area of the Southeast region, and the watersheds that contained TOC concentration data only represented 8 percent of total area of the Southeast region and 35 percent of the Southwest region.

Summertime concentrations were better represented in the concentration datasets than those collected in the winter. The Southeast, South-Central, Southwest, and Yukon regions had DIC concentrations collected through the year. However, nearly 80 percent of the DIC values and 65 percent of TOC values for the North Slope region were collected in June through August, with no TOC values for January, February, or March. Nearly 60 percent of DIC and TOC samples in the Northwest region were collected from June through August, which may have biased distributions of concentrations to represent more carbon transport via surface-water rather than groundwater flow.

In this assessment, the gas transfer velocity for $CO_2$ efflux calculation for rivers was not permitted to exceed 30 m/d based on equation 8.5. It is important to note that the model to estimate gas transfer velocity of $CO_2$ outlined in Raymond and others (2012) and used for this assessment was developed from a dataset that did not include any measurements from steep-slope or high-altitude locations and, as such, the results of this model in highly diverse landscapes should be interpreted with appropriate caution. Validation data to support evasion rates of this magnitude do not currently exist; however, recent research measuring oxygen transfer rates suggests that gas transfer velocities in the upper reaches of the Colorado River can range from 9 m/d in the large main channels up to 338 m/d in rapids (Hall and others, 2012).

The estimates of stream and river surface area for each hydrologic region ranged from 0.3 to 0.8 percent of the total area and are consistent with other published values (Aufdenkampe and others, 2011; Downing and others, 2012); however, remote sensing techniques could be used to further constrain the hydraulic geometry coefficients that are appropriate at the basin scale (Striegl and others, 2012). Specifically, there is a need to constrain the surface areas of first-order stream systems in headwater areas that may be poorly characterized within the EDNA dataset. The underlying 30-m digital elevation model used to define stream reaches is coarse, did not capture strong seasonal variation in flow, and had some inaccurate streamflow lines, particularly in low-elevation areas (Holmes and others, 2000).

The locations of USGS streamgages, which were used to calculate the hydraulic geometry coefficients, introduced a bias because they were placed in a location that was best suited for accurate discharge measurements (Leopold and Maddock, 1953; Park, 1977). Therefore, the locations most likely do not represent the entire range of variability in the relationships among stream depth, width, and velocity that exists for river channels across the State of Alaska. A wider range of variability of these stream geomorphology factors likely exists in Alaska because of the low levels of human development and lack of stream channelization or other flow restrictions.

Using the available data, we were not able to accurately model the effect of seasonality on estimated mean $CO_2$ emission from lacustrine or riverine systems (Rouse and others, 1997). In dimictic lakes (lakes that experience ice cover and mix completely in the spring and fall), $CO_2$ concentrations build up under ice cover and in the hypolimnetic bottom waters as a result of heterotrophic respiration and are degassed rapidly during mixing following ice melt (Michmerhuizen and others, 1996; Riera and others, 1999). In addition, boreal and arctic lakes are commonly shallow, resulting in a higher susceptibility to climate and seasonal shifts in temperature, reducing ice cover and increasing levels of light penetration to sediments, which could, in turn, influence the seasonality of dissolved $CO_2$ through biological metabolism and thermal stratification (Rouse and others, 1997; Smol and others, 2005). These aspects of the seasonal $pCO_2$ dynamics were not included in the estimates.

Changes in permafrost are likely to have effects on regional-scale hydrology (Osterkamp and others, 2000; Walvoord and others, 2012), particularly related to lake surface area. Lake surface area was a key component in the modeling of $CO_2$ emissions and carbon burial in lakes in this assessment. Some studies in regions with degrading permafrost have reported significant decreases in lake surface area extent (Riordan and others, 2006; Roach and others, 2013), whereas others report no substantial change in lake surface area for most lakes in a study region (Jones, Arp, and others, 2009; Rover and others, 2012). Regardless of the study, it is clear that accurate assessment of changes in lake surface area relies on proper treatment of both inter- and intra-annual time scales (Rover and others, 2012; Chen and others, 2013). However, a remote sensing data archive that can address both inter- and intra-annual variability in lake surface areas in continuous and discontinuous permafrost regions for the entire State of Alaska is currently not available. Given that the aquatic carbon flux results in this chapter represent long-term annual averages and that roughly half of the lake surface area lies in nonpermafrost regions of Alaska, the effect of changes in lake surface area on these regional results is expected to be minimal.

There were several important sources of uncertainty in the carbon burial estimates including (1) loss of sediment carbon to postdepositional mineralization at 100 years, (2) effects of within-basin variability of sedimentation rates, and (3) extrapolation of sedimentation rate and sediment carbon concentration data from a relatively small sample ($n=70$) of lakes to the larger population of lakes in Alaska (approximately 1 million). Loss of carbon in sediments because of mineralization occurs primarily in the top layers of sediments, where oxygen concentrations are highest (Sobek and others, 2009). This loss of carbon was partly compensated for by using an average carbon concentration for the sediment deposited during the previous 100 years, which typically was the top 5 to 15 cm of sediments. Additional research is needed to better account for variations in carbon burial efficiency in Alaskan lakes. Sediment focusing refers to the propensity for fine-grained sediment to accumulate preferentially in the deepest part of the lake (Davis and Ford, 1982). Alternatively, in calm-water lakes, where sediment redistribution is rare, littoral areas can have higher sedimentation rates because of highly productive macrophyte beds, high allochthonous subsidies nearshore, and (or) thermokarsting lake margins. The sediment focusing factor (the ratio of sedimentation at a specific location in a lake to average sedimentation in the lake) for lakes in Alaska varies widely and appears to be at least partly a function of lake morphometry, with steep-sided lakes having high sediment focusing factors. Focusing factors also can change over time, as young, steep-sided lakes fill in (Blais and Kalff, 1995). A study of eight high-elevation lakes in the Rocky Mountain and Glacier National Parks indicated that sediment focusing factors averaged $1.6 \pm 0.5$ (mean $\pm$ s.d.; 1 anomalous sample excluded) (Mast and others, 2010). Most of these lakes are in glacial cirques with high relief and have steeply sloping lake bottoms; thus, they may represent the upper end of the range of sediment focusing effects. If postdepositional sediment carbon mineralization and sediment focusing are important in Alaskan lakes, the estimated carbon burial rates are likely overestimated. Error in regression model predictions represents another source of uncertainty in carbon burial calculations. Although the MLR models for sedimentation rates and sediment carbon concentrations (key parameters in the carbon burial calculations) explained 70 to 75 percent of the variance in observed values, at least 25 to 30 percent of the variance remains unexplained. An additional concern is that the suite of lakes that was used to derive the MLR models was not selected randomly from the entire lake population, potentially biasing the model regressions; this deficiency could be at least partly addressed through additional sampling.

# 8.4. Results

## 8.4.1. Coastal Carbon Export From Riverine Systems

The total coastal carbon export for the State of Alaska was 18.3 TgC/yr (5th and 95th percentiles of 16.3 TgC/yr and 25.0 TgC/yr; table 8.1) with 70 percent of the export as inorganic carbon. The highest total carbon export was from the Yukon region, at 5.5 TgC/yr. Most of the flux is from the Yukon River, which had the single highest flux for any river in the State. The coastal flux from the Yukon River flows north through the Bering Strait to the Arctic Ocean.

The Southeast and South-Central regions exported similar magnitudes of carbon to the coast, 3.8 TgC/yr (5th and 95th percentiles of 3.4 TgC/yr and 5.3 TgC/yr), and 3.5 TgC/yr (5th and 95th percentiles of 3.1 TgC/yr and 5.0 TgC/yr), respectively (table 8.1). The Southwest region had a lower flux of 2.7 TgC/yr (5th and 95th percentiles of 2.2 TgC/yr and 3.4 TgC/yr). The Northwest and North Slope regions had the lowest annual carbon fluxes of 1.5 TgC/yr (5th and 95th percentiles of 1.3 TgC/yr and 3.4 TgC/yr) and 1.3 TgC/yr (5th and 95th percentiles of 0.9 TgC/yr and 2.3 TgC/yr), respectively.

To illustrate the connectivity between the aquatic fluxes and contributing terrestrial drainage area, we divided carbon fluxes by watershed area to produce a carbon yield. The estimated total carbon yields were by far the highest in the Southeast region at 36.7 $gC/m^2/yr$ (5th and 95th percentiles of 32.4 $gC/m^2/yr$ and 50.7 $gC/m^2/yr$; table 8.1). The second highest yields were in the South-Central region at 17.0 $gC/m^2/yr$ (5th and 95th percentiles of 15.1 $gC/m^2/yr$ and 24.0 $gC/m^2/yr$). The lowest carbon yields were in the North Slope region with 6.1 $gC/m^2/yr$ (5th and 95th percentiles of 4.3 $gC/m^2/yr$ and 11.5 $gC/m^2/yr$).

There was substantial variability in the mean runoff among the regions, with the greatest total runoff in the Southeast region at 3.4 meters per year (m/yr) (5th and 95th percentiles of 2.9 m/yr and 5.5 m/yr) and the smallest total runoff in the North Slope region at 0.3 m/yr (5th and 95th percentiles of 0.2 m/yr and 0.6 m/yr). The mean DIC concentration in the Yukon region of 18.7 mg/L (s.d. of 9.9 mg/L) was nearly three times higher than the estimated mean DIC concentration in the Southeast region, which was 6.6 mg/L (s.d. of 5.2 mg/L). The range of TOC concentrations were narrower, with the highest estimated mean concentration in the North Slope region at 8.5 mg/L (s.d. of 6.1 mg/L) and the lowest in the Southwest region at 2.4 mg/L (s.d. of 1.9 mg/L).

## 8.4.2. Carbon Dioxide Flux From Riverine Systems

Overall, median $pCO^2$ values ranged from 1,000 to 5,900 µatm across all stream orders and hydrologic regions, representing a gradient spanning 3 to 15 times the mean atmospheric $CO_2$ concentration. This suggests that streams and rivers in the State remain continuously supersaturated compared with atmospheric $CO_2$ concentrations. The highest median $pCO_2$ value by region was in the Northwest region at 3,100 µatm, whereas the lowest median $pCO_2$ value of 1,700 µatm was in the Southeast region. Measurements of dissolved $CO_2$ are defined by the pH, alkalinity, and temperature at the time of measurement, and the small sample size within the Northwest region affected these concentration distributions. Average median $pCO_2$ for the State of Alaska was 2,200 µatm, or 5.6 times the approximate atmospheric $CO_2$ concentration of 390 µatm.

Estimated stream and river surface area was 8,000 $km^2$ (5th and 95th percentiles of 7,600 $km^2$ and 8,300 $km^2$), representing about 0.5 percent of the total area of Alaska (table 8.3). The highest total stream surface area of 4,200 $km^2$ (5th and 95th percentiles of 4,100 $km^2$ and 4,400 $km^2$) was in the Yukon region, whereas the smallest total stream surface area

**Table 8.3.** Estimated river and stream surface area and vertical fluxes and yields of carbon dioxide from riverine systems in Alaska.

[Sites are those used in the calculation of estimated partial pressure of carbon dioxide ($pCO_2$). Values are estimates of the total median river and stream surface areas, fluxes, and yields (fluxes normalized to watershed areas), and those presented in parentheses represent associated errors at the 5th and 95th percentiles. Total yields were calculated by dividing the estimated total flux by the regional area. Units: $km^2$, square kilometer; TgC/yr, teragram of carbon per year; $gC/m^2/yr$, gram of carbon per square meter per year]

| Hydrologic region | Number of sites | River and stream surface area ($km^2$) | Estimated total carbon flux (TgC/yr) | Estimated total carbon yield ($gC/m^2/yr$) |
|---|---|---|---|---|
| Southeast | 242 | 486 (461, 512) | 3.9 (2.2, 5.8) | 37.3 (21.2, 55.6) |
| South-Central | 511 | 1,003 (947, 1,061) | 4.5 (2.5, 6.8) | 21.7 (12, 32.9) |
| Southwest | 166 | 1,235 (1,164, 1,307) | 3.1 (1.6, 5.0) | 10.5 (5.6, 17.3) |
| Yukon | 333 | 4,217 (4,063, 4,379) | 3.7 (2.0, 6.3) | 7.1 (3.7, 12) |
| Northwest | 81 | 507 (481, 533) | 0.8 (0.4, 1.3) | 4.2 (2.2, 7.1) |
| North Slope | 136 | 524 (496, 553) | 0.6 (0.3, 1.1) | 3.1 (1.7, 5.3) |
| **Total or mean** | **1,469** | **7,972 (7,612, 8,345)** | **16.6 (9.0, 26.3)** | **11.0 (6.0, 17.4)** |

was in the Southeast region at 490 km$^2$ (5th and 95th percentiles of 460 km$^2$ and 510 km$^2$). Stream and river surface area as a percentage of the landscape was largest in the Yukon region at 0.80 percent (5th and 95th percentiles of 0.77 percent and 0.83 percent), but only 0.26 percent (5th and 95th percentiles of 0.24 percent and 0.27 percent) across the North Slope region.

Total efflux of $CO_2$ from rivers in Alaska was 16.6 TgC/yr (5th and 95th percentiles of 9.0 TgC/yr and 26.3 TgC/yr) with the highest fluxes from the Yukon and South-Central regions at 3.7 TgC/yr (5th and 95th percentiles of 2.0 TgC/yr and 6.3 TgC/yr) and 4.5 TgC/yr (5th and 95th percentiles of 2.5 TgC/yr and 6.8 TgC/yr), respectively (table 8.3). The smallest efflux was estimated for the North Slope region at 0.6 TgC/yr (5th and 95th percentiles of 0.3 TgC/yr and 1.1 TgC/yr). Normalizing greenhouse-gas emissions to $CO_2$ equivalent using global warming potentials produced a total river efflux of 58.7 teragrams of carbon dioxide equivalent per year ($TgCO_2$-eq/yr) for the State of Alaska.

Carbon yield for the State of Alaska was 11.0 gC/m$^2$/yr (5th and 95th percentiles of 6.0 gC/m$^2$/yr and 17.4 gC/m$^2$/yr). The distribution of yield estimates across regions differed from the distribution of total flux estimates. Highest yield was estimated for the Southeast region at 37.3 gC/m$^2$/yr (5th and 95th percentiles of 21.2 gC/m$^2$/yr and 55.6 gC/m$^2$/yr), whereas the smallest yield was estimated for the North Slope region at 3.1 gC/m$^2$/yr (5th and 95th percentiles of 1.7 gC/m$^2$/yr and 5.3 gC/m$^2$/yr). In general, the range of yield estimates among the six regions of Alaska decreased with increasing latitude, where colder regions tended to have smaller yields primarily because of a larger proportion of defined ice cover throughout the year.

## 8.4.3. Carbon Dioxide Flux from Lacustrine Systems

Across the State, median lake $pCO_2$ concentrations ranged from 973 µatm, or 2 times atmospheric concentration, across the Yukon region to a high of 4,189 µatm, or nearly 10 times atmospheric concentration, in the Southwest region. These numbers represent high estimates for the dissolved $CO_2$ concentrations; however, limited measurements (n=1,329) may be contributing a bias to these calculations.

Overall, 1,019,224 individual lakes and reservoirs derived from the NHD dataset were used for this study, totaling 52,300 km$^2$ representing 4 percent of the State of Alaska (table 8.4). The proportion of lake area varied across each of the six hydrologic regions from a low of 2 percent in the Southeast region up to 7 percent in the Southwest region. This very high value of 7 percent is the result of a few very large lakes found within the Southwest region and is dominated by Lake Iliamna, which has a surface area of approximately 2,600 km$^2$.

Gas transfer velocities ($kCO_{2-lake}$) calculated using equation 8.6 averaged across regions did not vary significantly because of similarity in average wind speeds ($U_{10}$). Lowest $kCO_{2-lake}$ values were estimated for the Southeast region at 0.6 m/d, (s.d. of 0.04 m/d) ranging to a high of 0.8 m/d (s.d. of 0.1 m/d) for the Northwest region.

Total lake $CO_2$ emission was estimated to be 8.2 TgC/yr (5th and 95th percentiles of 6.1 TgC/yr and 11.2 TgC/yr; table 8.4). The highest lake efflux was estimated for the Southwest region at 5.8 TgC/yr (5th and 95th percentiles of 4.3 TgC/yr and 7.6 TgC/yr). The flux from this region was an order of magnitude larger than the remaining regions

**Table 8.4.** Estimated lake surface area and vertical fluxes and yields of carbon dioxide from lacustrine systems in Alaska.

[Sites are those used in the calculation of the partial pressure of carbon dioxide ($pCO_2$). Values are estimates of the total median lake surface areas, fluxes, and yields (fluxes normalized to watershed areas), and those presented in parentheses represent associated errors at the 5th and 95th percentiles. Total yields were calculated by dividing the estimated total flux by the regional area. Units: km$^2$, square kilometer; TgC/yr, teragram of carbon per year; gC/m$^2$/yr, gram of carbon per square meter per year]

| Hydrologic region | Number of sites | Lake surface area (km$^2$) | Estimated total carbon flux (TgC/yr) | Estimated total carbon yield (gC/m$^2$/yr) |
|---|---|---|---|---|
| Southeast | 44 | 1,587 | 0.3 (0.2, 0.4) | 3.2 (2.2, 3.8) |
| South-Central | 148 | 3,841 | 0.7 (0.6, 0.9) | 3.4 (2.8, 4.4) |
| Southwest | 214 | 20,946 | 5.8 (4.3, 7.6) | 19.8 (14.9, 26.1) |
| Yukon | 305 | 10,947 | 0.4 (0.2, 0.6) | 0.8 (0.4, 1.2) |
| Northwest | 46 | 4,069 | 0.4 (0.3, 0.8) | 2.1 (1.5, 4.3) |
| North Slope | 133 | 10,886 | 0.6 (0.5, 0.9) | 3.1 (2.2, 4.5) |
| **Total or mean** | **890** | **52,276** | **8.2 (6.1, 11.2)** | **5.5 (4.0, 7.4)** |

across Alaska. Lowest lake fluxes were estimated for the Southeast region at 0.3 TgC/yr (5th and 95th percentiles of 0.2 TgC/yr and 0.4 TgC/yr). Excluding the estimated flux for the Southwest, lake emission ranged from 0.3 to 0.7 TgC/yr across all other hydrologic regions. Normalizing greenhouse-gas emissions to $CO_2$ equivalent produced a total lake $CO_2$ emission of 30.1 $TgCO_2$-eq/yr (5th and 95th percentiles of 22.4 $TgCO_2$-eq/yr and 41.1 $TgCO_2$-eq/yr).

Average lake yield for the State of Alaska was 5.5 $gC/m^2/yr$ (5th and 95th percentiles of 4.0 $gC/m^2/yr$ and 7.4 $gC/m^2/yr$). Highest yield was estimated for the Southwest region at 19.8 $gC/m^2/yr$ (5th and 95th percentiles of 14.9 $gC/m^2/yr$ and 26.1 $gC/m^2/yr$), whereas the smallest yield was estimated for the Yukon region at 0.8 $gC/m^2/yr$ (5th and 95th percentiles of 0.4 $gC/m^2/yr$ and 1.2 $gC/m^2/yr$). Overall, the variation in both the total efflux and yield estimates among the regions was driven primarily by regional differences in the median lake $CO_2$ concentrations and total lake area.

## 8.4.4. Carbon Burial in Lacustrine Systems

Observed water body sedimentation rates at the cored lakes ranged from 0.1 to 5.3 millimeters per year (mm/yr) and had an exponential or log-normal distribution. The estimated median sedimentation rate for lakes of Alaska was 1.5 mm/yr, with the lowest rates in the Northwest and South-Central regions (0.4 mm/yr and 0.6 mm/yr); intermediate rates in the North Slope, Yukon, and Southeast regions (1.2 to 1.8 mm/yr); and highest rates in the Southwest region (2.3 mm/yr).

Observed sediment carbon concentrations at the cored lakes ranged from 0.6 to 30.7 percent (by dry weight) and were exponentially or log-normally distributed. The estimated median sediment carbon concentration in lakes of Alaska was 18.2 percent and were lowest in the Southeast, Southwest, and North Slope regions (16.6 to 17.7 percent); intermediate in the Northwest and South-Central regions (18.0 percent and 18.1 percent); and highest in the Yukon region (19.1 percent).

The median estimated total flux of carbon owing to burial in lakes of Alaska was –1.88 TgC/yr (5th and 95th percentiles of –1.03 TgC/yr and –2.82 TgC/yr), and values varied substantially among hydrologic regions (table 8.5). Estimated flux from carbon burial was smallest in the Southeast, Northwest, and South-Central regions (–0.05 to –0.10 TgC/yr); intermediate in the North Slope and Yukon regions (–0.33 TgC/yr and –0.46 TgC/yr, respectively); and greatest in the Southwest region (–0.88 TgC/yr). When normalized to the area of each hydrologic region (yield), the median estimated flux from carbon burial in lakes was –1.2 $gC/m^2/yr$ (5th and 95th percentile estimates of –0.7 $gC/m^2/yr$ and –1.9 $gC/m^2/yr$). Carbon burial yields were lowest in the Northwest, Southeast, and South-Central regions (–0.3 to –0.5 $gC/m^2/yr$); intermediate in the Yukon region (–0.9 $gC/m^2/yr$); and highest in the North Slope and Southwest regions (–1.6 $gC/m^2/yr$ and –3.0 $gC/m^2/yr$, respectively).

The estimated carbon burial rate normalized to water body area was –31 $gC/m^2/yr$ for Alaska, but the rates varied substantially among hydrologic regions. The Northwest and South-Central regions had the lowest estimated carbon burial rates (–8 $gC/m^2/yr$ and –11 $gC/m^2/yr$); the North Slope and Yukon regions had intermediate rates (–23 $gC/m^2/yr$ and –30 $gC/m^2/yr$); and the Southeast and Southwest regions had the highest rates (–36 $gC/m^2/yr$ and –44 $gC/m^2/yr$; table 8.5).

**Table 8.5.** Estimated carbon burial in lacustrine sediments in Alaska.

[Sites are those where carbon burial was calculated from sediment cores. Values are estimates of the total median fluxes, yields (fluxes normalized to watershed areas), and burial rates, and those presented in parentheses represent associated errors at the 5th and 95th percentiles. Carbon yields were calculated by dividing the estimated total flux divided by the hydrologic region area. Negative values represent sequestration. Units: TgC/yr, teragram of carbon per year; $gC/m^2/yr$, gram of carbon per square meter per year]

| Hydrologic region | Number of sites | Estimated total carbon flux (TgC/yr) | Estimated total carbon yield normalized to watershed area ($gC/m^2/yr$) | Estimated carbon burial rate normalized to water body area ($gC/m^2/yr$) |
|---|---|---|---|---|
| Southeast | 1 | –0.05 (–0.03, –0.07) | –0.5 (–0.3, –0.6) | –36 (–22, –50) |
| South-Central | 17 | –0.10 (–0.07, –0.13) | –0.5 (–0.3, –0.6) | –11 (–2, –22) |
| Southwest | 24 | –0.88 (–0.54, –1.24) | –3.0 (–1.9, –4.3) | –44 (–27, –63) |
| Yukon | 15 | –0.46 (–0.26, –0.64) | –0.9 (–0.5, –1.2) | –30 (–16, –44) |
| Northwest | 2 | –0.06 (–0.02, –0.12) | –0.3 (–0.1, –0.7) | –8 (–2, –23) |
| North Slope | 9 | –0.33 (–0.10, –0.62) | –1.6 (–0.5, –3.0) | –23 (–2, –47) |
| **Total or mean** | **68** | **–1.88 (–1.03, –2.82)** | **–1.2 (–0.7, –1.9)** | **–31 (–16, –49)** |

## 8.5. Discussion

The magnitude of carbon transported laterally, emitted, and stored in inland waters is controlled largely by variability in climate, hydrology, and exchanges of both inorganic and organic carbon among the terrestrial landscape, aquatic environments, and the atmosphere. The source of aquatic carbon is the combination of instream production and delivery of terrestrially derived carbon via surface-water or groundwater flow paths. Rising temperatures have already affected the large pools of carbon stored in the soils and permafrost (Striegl and others, 2007; Schuur and others, 2008; Frey and McClelland, 2009; Tarnocai and others, 2009) and have reduced the size of glaciers in Alaska (Arendt and others, 2002; Berthier and others, 2010). Therefore, it is important to provide accurate estimates of current carbon fluxes in aquatic environments, so that future effects of climate change can be determined.

### 8.5.1. Coastal Export and Carbon Dioxide Flux From Riverine Systems

The coastal carbon export from the Southeast and South-Central regions of Alaska accounted for approximately 40 percent of the State's total lateral flux at 7.3 TgC/yr. The lateral carbon yields from the Southeast region were the highest in the State at 36.7 $gC/m^2/yr$. The South-Central region had total carbon export nearly equivalent to that of the Southeast region; however, given its larger total area, the yields were lower (17.0 $gC/m^2/yr$). The mean annual precipitation for these regions, particularly along the coast, can be between 2 and 3 m, and in mountainous headwaters mean annual precipitation can be a great as 8 m (Powell and Molnia, 1989). Heavy precipitation produces an abundance of small, swift-moving streams. For the Southeast region, the estimated magnitude of total discharge was 356 cubic kilometers per year ($km^3/yr$), which translates to a runoff of 3.4 m/yr. Total discharge for the South-Central region was 220 $km^3/yr$, which translates to a water yield of 1.1 m/yr (5th and 95th percentiles of 0.8 m/yr and 2.5 m/yr).

Forested and wetland soils in the Southeast and South-Central regions of Alaska deliver organic carbon to streams draining to the coast (Fellman and others, 2008; D'Amore and others, 2010), and mean organic carbon concentrations for these regions were between 3 and 4 mg/L. The organic carbon fluxes estimated within this report are comparable with other estimates for this region (D'Amore and others, 2015). With substantial ice cover in these two regions, glacial runoff is a significant source of organic carbon (Hood and others, 2009; Schroth and others, 2011) and inorganic carbon, as considerable rock weathering occurs under ice sheets (Ludwig and others, 1999). Mean inorganic carbon concentrations for rivers and streams were 6.6 mg/L and 11 mg/L for the Southeast and South-Central regions, respectively.

Estimated riverine $CO_2$ efflux from the Southeast and South-Central regions was over 50 percent of the total vertical $CO_2$ emission for the State of Alaska at 8.4 TgC/yr, yet these regions only account for 19 percent of the total water area. These two regions had very high yield estimates—from 21.7 $gC/m^2/yr$ for the South-Central region to 37.3 $gC/m^2/yr$ for the Southeast region. Average gas transfer velocities in this region were the highest in the State at approximately 24 m/d. Although this is within published estimates of stream $kCO_2$ (Hall and others, 2012; Huotari and others, 2013), it remains unclear if riverine $CO_2$ emissions can be maintained with transfer rates this high. To date, there are no comparable vertical $CO_2$ emissions from riverine systems for these two regions.

The coastal carbon export combined with $CO_2$ emissions produced a river carbon flux of 5.8 TgC/yr from the Southwest region. This region had a high percent of total carbon flux as DIC (78.4 percent). This is likely due to the sedimentary rocks rich in carbonates that underlie this region (Dürr and others, 2005), and the Kuskwokwim River has significantly affected the carbonate saturation indices of the Bering Sea (Mathis and others, 2011). Currently, there are no other studies that can be used as a comparison for the estimates from this region.

Carbon cycling and storage at high latitudes have been key issues in carbon cycle science. Therefore, estimates of aquatic carbon fluxes exist for major watersheds draining to the Arctic Ocean, including the Yukon River and several of the main rivers draining the North Slope of Alaska (Colville, Kuparuk, and Sagavanirktok Rivers). The results presented in this chapter support many of these existing flux estimates.

The highest lateral carbon fluxes for Alaska, estimated at 5.5 TgC/yr, were in the Yukon River Basin, likely owing to high discharge (125 $km^3/yr$), DIC concentration (18.6 mg/L, s.d. of 10.0 mg/L), and TOC concentration (4.8 mg/L, s.d. of 10.0 mg/L). This estimate is about 35 percent lower than previous Yukon River carbon flux estimates of 7.2 TgC/yr (Striegl and others, 2007), in part because of the difference in the period of record between the two studies. This report used data from 1975 to 2013 to calculate fluxes for the Yukon River at Pilot Station (NWIS station ID=15565447), but Striegl and others (2007) only used data between 2001 and 2005. The water chemistry data for these two different studies were comparable. The median alkalinity as calcium carbonate for the Yukon River at Pilot Station was 76.2 mg/L in this assessment compared with 74.5 mg/L of Striegl and others (2007). The median alkalinity as DOC was 5.6 mg/L in this assessment compared with 5.5 mg/L of Striegl and others (2007). However the median discharge of 125 $km^3/yr$ in this report was much lower than 146 $km^3/yr$ for the time period used in Striegl and others (2007). The 17-percent difference in discharge is likely the main cause for different flux estimates between the two studies.

In this assessment, riverine $CO_2$ emission from the Yukon region was estimated to be 3.7 TgC/yr (5th and 95th percentiles of 2.0 TgC/yr and 6.3 TgC/yr), which is lower compared

with 7.7 TgC/yr (5th and 95th percentiles of 6.7 TgC/yr and 9.2 TgC/yr) of Striegl and others (2012; herein called Striegl and others). In this report, the yield estimate for the Yukon region was 7.1 gC/m$^2$/yr (5th and 95th percentiles of 3.7 gC/m$^2$/yr and 12.0 gC/m$^2$/yr), which is lower than 10.5 g/C/m$^2$/yr (5th and 95th percentiles of 9.0 gC/m$^2$/yr and 13.0 gC/m$^2$/yr) of Striegl and others, although their value falls within our error estimate.

Multiple factors contributed to the difference in total river evasion estimates between the two studies. Striegl and others included the total efflux for the Canadian proportion of the Yukon River Basin, whereas this study presents fluxes only for the portion of the basin within the Alaskan State boundary. The area of the Yukon River Basin within the State of Alaska estimated in this report was approximately 530,000 km$^2$, which represents 60 percent of the total Yukon River Basin. Additionally, Striegl and others used high-resolution remote sensing methods to determine stream and river surface area for all but the smaller tributaries and estimated a total river surface area of 10,000 km$^2$, which is 1.2 percent of the total land area in the Yukon River Basin. In this report, the water surface area was lower, about 0.8 percent of the land area, because EDNA did not adequately represent low-order streams.

Another methodological difference between the two studies was that this report used modeled estimates for $kCO_{2-river}$ that ranged from 2.5 to 28.0 m/d from first through tenth stream orders for the Yukon River according to methods outlined in Zhu and Reed (2014), but the maximum $kCO_{2-river}$ used by Striegl and others approached 6.9 m/d with a minimum of 0.3 m/d along the main stem of the upper Yukon River Basin. In addition, Striegl and others estimated a total of 200 days, or 54 percent of the year, where no efflux occurred based on ice cover conditions; this was applied uniformly across the basin to the total flux estimate. In this report, ice cover was estimated spatially using mean monthly temperature to produce a range of 145 to 152 days that are ice free depending upon topographic location. Thus, this report presents higher flux rates for shorter periods of time and for less surface area compared with Striegl and others. Because of the difference in methods between the two studies, identification of $CO_2$ emission hotspots also diverged. The methods used to derive the $CO_2$ emission estimates from rivers presented in this report indicated that the dominant fluxes occurred either in the smaller tributaries or the highest order main stem of the river network determined by $kCO_{2-river}$ or by area, respectively. In contrast, Striegl and others suggest that the majority of the efflux occurs within the tributaries only. Despite these methodological differences, if we increase our flux by the increased proportion of surface area suggested by Striegl and others, we obtain a yield of 9.6 gC/m$^2$/yr, which is very similar to their 10.5 gC/m$^2$/yr.

Despite relatively high DIC (14.7 mg/L) and TOC concentrations (8.5 mg/L), the North Slope region had a low coastal carbon export rate of 1.3 TgC/yr, likely owing to relatively low discharge of 53 km$^3$/yr. This region had the highest TOC concentrations and the highest regional value of total carbon flux as TOC (38 percent). The summed organic carbon flux estimate for the Sagavanirktok, Kuparuk, and Colville Rivers in the North Slope region presented in this report was 0.41 TgC/yr (5th and 95th percentiles of 0.05 TgC/yr and 0.8 TgC/yr), which encompassed the McClelland and others (2014) estimate of 0.30 TgC/yr (s.d. of 0.03 TgC/yr) for the same rivers. Overall, the Northwest region is one of the most data-poor regions in the State, and this report presents the first estimates for river coastal carbon flux from this region of 1.5 TgC/yr.

The riverine $CO_2$ effluxes for the North Slope and Northwest regions were estimated to be 0.6 TgC/yr and 0.8 TgC/yr with yields of 3.1 gC/m$^2$/yr and 4.2 gC/m$^2$/yr, respectively. These regions represent only 10 percent of the total statewide riverine efflux, and the flux was driven primarily by a short ice-free period, averaging a total of 113 to 138 days, and by small surface areas of streams and rivers, representing only 0.26 percent of the land surface area in the North Slope region and 0.29 percent in the Northwest region. These yield estimates are larger than those derived from within the Kuparuk River watershed as part of the Toolik Lake LTER (Kling and others, 1992, 2000). At 3.8 gC/m$^2$/yr, this report's value is double the estimate for the Kuparuk River network of 1.7 gC/m$^2$/yr derived for 1994 through 1996 (Hobbie and Kling, 2014) and significantly higher than a more recent estimate for the same watershed of 0.02 gC/m$^2$/yr (Cory and others, 2014). Cory and others (2014) estimated the proportion of the landscape as stream and river surface to be about 0.23 percent, which is similar to this report's estimate, although it remains unclear how they estimated lateral inputs of DIC contributing to $pCO_2$ in their study, possibly biasing their total flux to be low.

## 8.5.2. Carbon Dioxide Flux From and Carbon Burial in Lacustrine Systems

The Southeast and South-Central regions showed nearly identical lake vertical flux estimates at 3.2 gC/m$^2$/yr and 3.4 gC/m$^2$/yr, respectively. To our knowledge, these are the first estimates for lake efflux in coastal regions that include temperate rainforest ecosystems. The calculated $pCO_2$ values were nearly identical across both the Southeast and South-Central regions at about 2,600 µatm. Input of organic carbon from forested and wetland systems may affect lake $pCO_2$ estimates, as median alkalinity estimates for the Southeast region were very low at around 2 mg/L, whereas median pH was 6.7 (David D'Amore, U.S. Department of Agriculture, Forest Service, written commun., November 3, 2014). A complication for modeling the efflux of $CO_2$ from lake ecosystems within these regions is the lack of data from central lake locations. Nearly all identified sites in the Southeast region of Alaska are from samples taken at either inlet or

outlet of a lake. These concentrations are likely to be different than the carbon concentrations at central points within the lake, where the greatest turbulence and greatest gas emission rates likely occur.

A very high lake $CO_2$ emission of 5.8 TgC/yr was calculated for the Southwest region. This value is larger than all other regions in Alaska combined. The median estimated $pCO_2$ value for this region was 4,200 µatm, with values ranging between 19 and 71,000 µatm. There are currently no published estimates of direct measurements of lake $CO_2$ concentrations within this region for comparison. Direct measurements refer to in situ monitoring of $CO_2$ with a type of infrared sensor, as opposed to the indirect measurement used in this report by estimating $CO_2$ concentrations from alkalinity, pH, and temperature measurements. Unpublished direct dissolved $CO_2$ measurements for small lakes near Lake Iliamna had a maximum $pCO_2$ of 2,800 µatm and were undersaturated (<390 µatm) for half of the period that the lake was covered with ice (G. Holtgrieve, University of Washington-Seattle, written commun.). In addition to the high concentration of dissolved $CO_2$ identified within the Southwest region, this region also has significantly higher lake surface area at 21,000 $km^2$, nearly double the estimates for the Yukon and North Slope regions. Obtaining direct dissolved $CO_2$ concentration measurements from multiple points on large lakes is critical to reducing the uncertainty for the high estimated lake carbon emissions in this region.

Current research on boreal and arctic lakes consistently show annual dissolved $CO_2$ concentrations to be in excess of atmospheric $CO_2$ (Huttunen and others, 2003; Sobek and others, 2005; Jonsson and others, 2008). In lakes across the boreal and arctic regions of Alaska, including the North Slope, Northwest, and Yukon regions, median $pCO_2$ values ranged from about 970 µatm in the Yukon to about 1,900 µatm in the Northwest. Much of the $CO_2$ supersaturation is hypothesized to originate from the mineralization of both allochthonous and autochthonous carbon sources (Roehm and others, 2009; Solomon and others, 2013). However, although DOC correlates with dissolved $CO_2$ values, significant regional variation exists so that a model that can be applied across the circumboreal region is still not available (Roehm and others, 2009).

For this study, the North Slope lake efflux was estimated to be 0.6 TgC/yr (5th and 95th percentiles of 0.5 TgC/yr and 0.9 TgC/yr), resulting in a flux of 3.1 $gC/m^2/yr$ (5th and 95th percentiles of 2.2 $gC/m^2/yr$ and 4.5 $gC/m^2/yr$). Previous lake studies at the Toolik Lake LTER estimated fluxes of 1.1 $gC/m^2/yr$ (Hobbie and Kling, 2014) and 0.4 $gC/m^2/yr$ (Cory and others, 2014). These flux measurements, made at a single site, were estimated with data from two different time periods—1994 through 1996 for the Hobbie and Kling study and 2001 through 2013 for the Cory and others study. These differences indicate that there is significant temporal variation in carbon fluxes within the Arctic. The lake $CO_2$ emissions estimated for the North Slope region in this study may be high owing to high initial DIC concentrations derived from the calculation of $pCO_2$ from ancillary data and because the timing of samples taken for this analysis may not be representative of the influence that seasonal hydrology and in situ primary production impart on carbon concentrations (Huttunen and others, 2003).

For lakes in the Yukon Flats area, the lake $CO_2$ emissions were estimated with direct dissolved $CO_2$ concentrations (Halm and Guldager, 2013; Halm and Griffith, 2014). The Yukon region's average $pCO_2$ values were the lowest across all regions, and the median value of 970 µatm was considerably lower than the next closest median $pCO_2$ value of 1,400 µatm, which was calculated for the North Slope region. The Yukon Flats data represent only single measurements, usually made during the summer, and significant seasonal fluctuations in these values are likely. Additional direct seasonal measurements of $CO_2$ concentrations for lakes throughout Alaska are necessary to determine if (1) low $pCO_2$ values are representative of lakes in other regions and (2) low concentrations persist even under seasonal fluctuations of in-lake biological processes, including photosynthesis and respiration.

The average sedimentation rate observed in Alaskan lakes (1.5 mm/yr) was similar to those from a study of lakes in eastern North America, which reported that historical sedimentation rates had a log-normal distribution, with a median of 2.2 mm/yr (Webb and Webb, 1988). A few studies have reported sedimentation rates for Alaskan lakes: Cornwell (1985) reported a sediment accumulation rate of 0.16 mm/yr for Toolik Lake, in the foothills of the North Slope region, and noted that low rainfall, a short runoff period, and stabilization of soils by thick organic matter layers and nearly continuous tundra vegetation contribute to low sedimentation rates in the lake. Higher sedimentation rates (2.5 mm/yr) were reported for Black Lake, on the Alaskan Peninsula, which receives more precipitation and is covered in dense forest, rather than tundra vegetation (Post, 2011).

Sediment carbon concentrations for Alaskan lakes were similar to those documented for 3 oligotrophic, humic-rich lakes in Sweden (21 to 31 percent; Sobek and others, 2009, 2014), 16 lakes in western Ontario (20 percent, s.d. of 7 percent), and 23 lakes in Wisconsin (20 percent, s.d. of 10 percent) (Brunskill and others, 1971). In contrast, sediment carbon concentrations were much lower in seven lakes in western Greenland (1.8 to 8.9 percent); the study area was cold and dry, with a mean annual temperature of –6 °C and mean annual precipitation of 150 mm/yr (Sobek and others, 2014); sparse vegetation and poorly developed soils may have limited contributions of organic matter to the lakes from the surrounding terrestrial environment.

Variations in carbon burial rate in Alaska reflect differences in sedimentation rate, sediment carbon concentration, and the extent of water bodies (see equation 8.7). Based on results from the stepwise MLR modeling, sedimentation rates were strongly related to land-cover type, with shrubland,

mixed forest, and herbaceous wetland exerting a positive influence and permafrost exerting a negative influence (table 8.6). The positive influence of shrubland on sedimentation rates may reflect the susceptibility of this land-cover type to erosion, whereas the positive influence of mixed forest and herbaceous wetlands may be related to high productivity of vegetation in these areas. In addition, shrub distribution in tundra terrain is often confined to recently eroded gullies and water-track habitats, which may indicate recent erosion (Tape and others, 2011). The negative influence of permafrost on sedimentation rates probably is due to low erosion rates of frozen soil, except in areas with thermokarst where erosion can be important (Osterkamp and others, 2000). Differences in estimated sedimentation rates among regions reflect the relative abundance of land-cover types and permafrost. Low estimated sedimentation rates in the Northwest region, for example, may be attributed to the importance of permafrost, which underlies over 70 percent of the landscape in this region (chapter 3 of this report; Pastick, Jorgenson, and others, 2014). Relatively high sedimentation rates were estimated for the Southwest region, which has abundant shrubland and herbaceous wetlands and relatively little permafrost.

The stepwise MLR modeling indicated that sediment carbon concentrations were strongly related to log water body surface area, mean basin elevation, and percent of basin covered by bogs (table 8.6). Sediment carbon concentrations were inversely related to water body surface area, reflecting relatively high productivity rates in the littoral zone of lakes compared to deeper water zones; small lakes typically are shallower than large lakes, and littoral zones constitute a greater percentage of total lake area (Wetzel, 2001). Mean basin elevation also was a negative influence on sediment carbon concentration, probably because of decreases in primary productivity and associated soil organic carbon with elevation (Jobbágy and Jackson, 2000; Ping and others, 2008). Bogs were a positive influence on sediment carbon, as expected given the high organic carbon content of bog soils that have the potential for providing carbon subsidies to nearby lakes (Jobbágy and Jackson, 2000; Pastick, Rigge, and others, 2014).

The carbon burial rate estimated for Alaskan lakes in this study normalized to lake area (–31 $gC/m^2/yr$) is higher than long-term (Holocene) rates for boreal lakes in northern Quebec (–3.8 $gC/m^2/yr$; Ferland and others, 2012) and Finland (–0.2 to –8.5 $gC/m^2/yr$; Kortelainen and others, 2004); however, our estimates pertain only to the past 100 years. The carbon burial rates estimated herein for Alaska approach those in thermokarst lakes in Siberia (–47±10 $gC/m^2/yr$), which are relatively high because of thermokarst erosion, which contributes organic matter and nutrients to lakes, and cold temperatures, which limit decomposition (Walter Anthony and others, 2014). At the global scale, Dean and Gorham (1998) noted an inverse relation between carbon burial rates and lake area and estimated an average carbon accumulation rate of –5 $gC/m^2/yr$ for large lakes and –72 $gC/m^2/yr$ for small lakes; an inverse relation between carbon burial rates and lake size was observed in the present study as well.

Variations in estimated total carbon burial fluxes (in TgC/yr) among hydrologic regions primarily reflect differences in sedimentation rates and the areal extent of water bodies; these parameters showed much more variability among regions than sediment carbon concentrations, as indicated by the coefficient of variation (CV) for each parameter. The CV for sedimentation rates and water body area were 0.51 and 0.14, whereas the CV for sediment carbon concentrations was only 0.04. The Southwest region had the highest carbon burial rates among the regions of Alaska (table 8.5); this region also had greatest water body surface area (table 8.4) and the highest sedimentation rates. In contrast, carbon burial in lakes of the South-Central and Northwest regions was much smaller (table 8.5), reflecting lower water body surface areas (table 8.4) and sedimentation rates.

**Table 8.6.** Estimates, standard error of estimates, and p-values for independent variables used in multiple-linear-regression models for sedimentation rates and sediment carbon concentrations in Alaskan water bodies.

[$km^2$, square kilometer; m, meter]

| Independent variable | Sedimentation rate model | | | | | Sediment carbon concentration model | | | |
|---|---|---|---|---|---|---|---|---|---|
| | Intercept | Mixed forest (percent) | Shrubland (percent) | Herbaceous wetland (percent) | Permafrost (percent) | Intercept | Log lake area ($km^2$) | Mean elevation (m) | Bogs (percent) |
| Estimate | –0.0117 | 0.0161 | 0.0017 | 0.0126 | –0.0013 | 10.838 | –3.2805 | –0.0093 | 0.3781 |
| Standard error of estimate | –0.0117 | 0.0161 | 0.0017 | 0.0126 | –0.0013 | 1.0039 | 0.5014 | 0.0016 | 0.0518 |
| p-value | 0.63 | <0.0001 | <0.0001 | <0.0001 | 0.0008 | <0.0001 | <0.0001 | <0.0001 | <0.0001 |

## 8.6. Summary and Conclusions

The total statewide carbon flux from inland waters (coastal export plus $CO_2$ emissions from rivers and lakes minus burial in sediments) was 41.2 TgC/yr, and total carbon yields were 27.5 gC/m$^2$/yr. The greenhouse-gas-emission estimates reported in this chapter may be low because methane ($CH_4$) fluxes were not included owing to a lack of lacustrine and riverine $CH_4$ concentration data across Alaska. Recent studies have documented that both $CO_2$ and $CH_4$ may represent a consistent carbon loss pathway from aquatic ecosystems to the atmosphere (Walter and others, 2007; Crawford and others, 2013; Sepulveda-Jauregui and others, 2014). Using the lake $CH_4$ estimates for northern latitudes (Wik and others, 2016) and applying them to the lake surface area of Alaska indicates that lake $CH_4$ emissions may equal 0.5 TgC/yr. Current modeling efforts strive to integrate $CH_4$ concentration samples from a variety of lake types, including deep glacial lakes as well as thermokarst water bodies in Alaska, as well as low- and high-order streams and rivers in order to provide an accurate estimate of current lake and river $CH_4$ emissions in Alaska.

There was considerable variability in the estimated inland waters' carbon fluxes among the six hydrologic regions in Alaska. The Southeast region, with high precipitation rates and an abundance of short, steep streams, had the highest total yield (flux divided by hydrologic area) in the State at 76.7 gC/m$^2$/yr. The South-Central region had the second highest total yield of 41.6 gC/m$^2$/yr. The Southwest region had the highest lake surface area (nearly 21,000 km$^2$) and the highest lake $CO_2$ emission rates (5.8 TgC/yr), which contributed to the relatively high overall yield of 36.5 gC/m$^2$/yr. The Yukon region had a total yield of 17.5 gC/m$^2$/yr. Both the Northwest and the North Slope regions, with the lowest temperatures and precipitation among the six regions, had the smallest overall combined yields of 14.7 gC/m$^2$/yr and 10.7 gC/m$^2$/yr, respectively.

This chapter focused on presenting results of current carbon fluxes from inland aquatic systems, but projected climate changes are likely to influence the magnitude of aquatic carbon fluxes in future decades. Predicted changes to the hydrologic cycle include increased streamflow in high-latitude regions (Hinzman and others, 2005; Brabets and Walvoord, 2009) and increased runoff owing to increased rates of glacier melt (Arendt and others, 2002). The influence of groundwater on regional hydrology is also likely to change because of permafrost thaw (Walvoord and others, 2012). Increased forest fires (Kasischke and others, 2010), permafrost thaw (Walvoord and Striegl, 2007; Tank, Frey, and others, 2012), and changes in vegetation composition (Chapin and others, 1995) are all likely to affect the amount and composition of carbon delivered to aquatic systems. Coupling both hydrologic and biogeochemical reactions over space and time will be key to accurately predicting changes in the magnitude of aquatic carbon fluxes in the future.

The results presented in this chapter indicate that the magnitude of inland waters' aquatic carbon fluxes is significant at 41.2 TgC/yr. Since the models that produced the soil $CO_2$ flux estimates in the assessment were not coupled with the models that produced the riverine inorganic carbon flux or the vertical $CO_2$ emissions, the appropriate amount of $CO_2$ that is emitted from the aquatic ecosystems was not subtracted from the heterotrophic respiration term, which may lead to double counting. Additionally, if the DOC leaching from soil organic matter pools was not adequately represented within the terrestrial modeling environment, the modeled soil pools could be amassing organic carbon that has actually been transported, processed, or stored in aquatic ecosystems. Development of a model framework that couples the terrestrial and aquatic carbon processing and transport is key to understanding whether terrestrial landscapes represent a dominant source of carbon to freshwater systems. Chapter 9 of this report will present a complete picture of terrestrial and aquatic ecosystems and will illustrate a comparison that indicates that the linkage between these two environments is important to understand fully the role they play in greenhouse-gas storage and cycling.

## 8.7. References Cited

Abbott, M.B., Edwards, M.E., and Finney, B.P., 2010, A 40,000-yr record of environmental change from Burial Lake in northwest Alaska: Quaternary Research, v. 74, no. 1, p. 156–165, http://dx.doi.org/10.1016/j.yqres.2010.03.007.

Abbott, M.B., Finney, B.P., Edwards, M.E., and Kelts, K.R., 2000, Lake-level reconstructions and paleohydrology of Birch Lake, central Alaska, based on seismic reflection profiles and core transects: Quaternary Research, v. 53, no. 2, p. 154–166, http://dx.doi.org/10.1006/qres.1999.2112.

Akaike, Hirotugu, 1981, Likelihood of a model and information criteria: Journal of Econometrics, v. 16, no. 1, p. 3–14, http://dx.doi.org/10.1016/0304-4076(81)90071-3.

Anderson, D.E., Striegl, R.G., Stannard, D.I., Michmerhuizen, C.M., McConnaughey, T.A., and LaBaugh, J.W., 1999, Estimating lake-atmosphere $CO_2$ exchange: Limnology and Oceanography, v. 44, no. 4, p. 988–1001, http://dx.doi.org/10.4319/lo.1999.44.4.0988.

Anderson, Lesleigh, Abbott, M.B., and Finney, B.P., 2001, Holocene climate inferred from oxygen isotope ratios in lake sediments, central Brooks Range, Alaska: Quaternary Research, v. 55, no. 3, p. 313–321, http://dx.doi.org/10.1006/qres.2001.2219.

Arendt, A.A., Echelmeyer, K.A., Harrison, W.D., Lingle, C.S., and Valentine, V.B., 2002, Rapid wastage of Alaska glaciers and their contribution to rising sea level: Science, v. 297, no. 5580, p. 382–386, http://dx.doi.org/10.1126/science.1072497.

Aufdenkampe, A.K., Mayorga, Emilio, Raymond, P.A., Melack, J.M., Doney, S.C., Alin, S.R., Aalto, R.E., and Yoo, Kyungsoo, 2011, Riverine coupling of biogeochemical cycles between land, oceans, and atmosphere: Frontiers in Ecology and the Environment, v. 9, no. 1, p. 53–60, http://dx.doi.org/10.1890/100014.

Axford, Yarrow, and Kaufman, D.S., 2004, Late glacial and Holocene glacier and vegetation fluctuations at Little Swift Lake, southwestern Alaska, U.S.A.: Arctic, Antarctic, and Alpine Research, v. 36, no. 2, p. 139–146, http://dx.doi.org/10.1657/1523-0430(2004)036[0139:LGAHGA]2.0.CO;2.

Barto, David, 2004, Assessing the production of sockeye salmon (*Oncorhynchus nerka*) at Chilkat Lake, southeast Alaska, using current trophic conditions and the paleolimnologic sediment record: Fairbanks, Alaska, University of Alaska, M.S. thesis, 111 p.

Berthier, E., Schiefer, E., Clarke, G.K.C., Menounos, B., and Rémy, F., 2010, Contribution of Alaskan glaciers to sea-level rise derived from satellite imagery: Nature Geoscience, v. 3, no. 2, p. 92–95, http://dx.doi.org/10.1038/ngeo737.

Bird, B.W., Abbott, M.B., Finney, B.P., and Kutchko, Barbara, 2009, A 2000 year varve-based climate record from the central Brooks Range, Alaska: Journal of Paleolimnology, v. 41, no. 1, p. 25–41, http://dx.doi.org/10.1007/s10933-008-9262-y.

Blais, J.M., and Kalff, Jacob, 1995, The influence of lake morphometry on sediment focusing: Limnology and Oceanography, v. 40, no. 3, p. 582–588, http://dx.doi.org/10.4319/lo.1995.40.3.0582.

Brabets, T.P., and Walvoord, M.A., 2009, Trends in streamflow in the Yukon River Basin from 1944 to 2005 and the influence of the Pacific Decadal Oscillation: Journal of Hydrology, v. 371, nos. 1–4, p. 108–119, http://dx.doi.org/10.1016/j.jhydrol.2009.03.018.

Brady, S.M., 2013, A multi-proxy approach to late quaternary environmental change at Little Harding Lake, interior Alaska: Pocatello, Idaho, Idaho State University, M.S. thesis, 157 p.

Brunskill, G.J., Povoledo, D., Graham, B.W., and Stainton, M.P., 1971, Chemistry of surface sediments of sixteen lakes in the Experimental Lakes Area, northwestern Ontario: Journal of the Fisheries Research Board of Canada, v. 28, no. 2, p. 277–294, http://dx.doi.org/10.1139/f71-038.

Butman, David, and Raymond, P.A., 2011, Significant efflux of carbon dioxide from streams and rivers in the United States: Nature Geoscience, v. 4, no. 12, p. 839–842, http://dx.doi.org/10.1038/ngeo1294.

Carlson, L.J., and Finney, B.P., 2004, A 13,000-year history of vegetation and environmental change at Jan Lake, east-central Alaska: The Holocene, v. 14, no. 6, p. 818–827, http://dx.doi.org/10.1191/0959683604hl762rp.

Chapin, F.S., III, Shaver, G.R., Giblin, A.E., Nadelhoffer, K.J., and Laundre, J.A., 1995, Responses of arctic tundra to experimental and observed changes in climate: Ecology, v. 76, no. 3, p. 694–711, http://dx.doi.org/10.2307/1939337.

Charlton, S.R., Parkhurst, D.L., and Appelo, C.A.J., 2014, Phreeqc—R interface to geochemical modeling software (ver. 3): U.S. Geological Survey, accessed July 1, 2014, at http://cran.r-project.org/web/packages/phreeqc/index.html.

Chen, Min, Rowland, J.C., Wilson, C.J., Altmann, G.L., and Brumby, S.P., 2013, The importance of natural variability in lake areas on the detection of permafrost degradation; A case study in the Yukon Flats, Alaska: Permafrost and Periglacial Processes, v. 24, no. 3, p. 224–240, http://dx.doi.org/10.1002/ppp.1783.

Chipman, M.L., Clarke, G.H., Clegg, B.F., Gregory-Eaves, Irene, and Hu, F.S., 2009, A 2000 year record of climatic change at Ongoke Lake, southwest Alaska: Journal of Paleolimnology, v. 41, no. 1, p. 57–75, http://dx.doi.org/10.1007/s10933-008-9257-8.

Chipman, M.L., Clegg, B.F., and Hu, F.S., 2012, Variation in the moisture regime of northeastern interior Alaska and possible linkages to the Aleutian Low; Inferences from a late-Holocene $\delta^{18}O$ record: Journal of Paleolimnology, v. 48, no. 1, p. 69–81, http://dx.doi.org/10.1007/s10933-012-9599-0.

Clegg, B.F., and Hu, F.S., 2010, An oxygen-isotope record of Holocene climate change in the south-central Brooks Range, Alaska: Quaternary Science Reviews, v. 29, nos. 7–8, p. 928–939, http://dx.doi.org/10.1016/j.quascirev.2009.12.009.

Cohn, B.R., 2009, Recent paleoenvironmental changes recorded in three non-anadromous lakes in southwest Alaska; Effects of climatic and vegetation dynamics on lake productivity: Fairbanks, Alaska, University of Alaska, M.S. thesis, 121 p.

Cole, J.J., and Caraco, N.F., 1998, Atmospheric exchange of carbon dioxide in a low-wind oligotrophic lake measured by the addition of $SF_6$: Limnology and Oceanography, v. 43, no. 4, p. 647–656, http://dx.doi.org/10.4319/lo.1998.43.4.0647.

Cole, J.J., Prairie, Y.T., Caraco, N.F., McDowell, W.H., Tranvik, L.J., Striegl, R.G., Duarte, C.M., Kortelainen, P., Downing, J.A., Middelburg, J.J., and Melack, J., 2007, Plumbing the global carbon cycle; Integrating inland waters into the terrestrial carbon budget: Ecosystems, v. 10, no. 1, p. 171–185, http://dx.doi.org/10.1007/s10021-006-9013-8.

Cornwell, J.C., 1985, Sediment accumulation rates in an Alaskan arctic lake using a modified $^{210}$Pb technique: Canadian Journal of Fisheries and Aquatic Sciences, v. 42, no. 4, p. 809–814, http://dx.doi.org/10.1139/f85-103.

Cory, R.M., Ward, C.P., Crump, B.C., and Kling, G.W., 2014, Sunlight controls water column processing of carbon in arctic fresh waters: Science, v. 345, no. 6199, p. 925–928, http://dx.doi.org/10.1126/science.1253119.

Crawford, J.T., Striegl, R.G., Wickland, K.P., Dornblaser, M.M., and Stanley, E.H., 2013, Emissions of carbon dioxide and methane from a headwater stream network of interior Alaska: Journal of Geophysical Research; Biogeosciences, v. 118, no. 2, p. 482–494, http://dx.doi.org/10.1002/jgrg.20034.

D'Amore, D.V., Edwards, R.T., Herendeen, P.A., Hood, Eran, and Fellman, J.B., 2015, Dissolved organic carbon fluxes from hydropedologic units in Alaskan coastal temperate rainforest watersheds: Soil Science Society of America Journal, v. 79, no. 2, p. 378–388, http://dx.doi.org/10.2136/sssaj2014.09.0380.

D'Amore, D.V., Fellman, J.B., Edwards, R.T., and Hood, Eran, 2010, Controls on dissolved organic matter concentrations in soils and streams from a forested wetland and sloping bog in southeast Alaska: Ecohydrology, v. 3, no. 3, p. 249–261, http://dx.doi.org/10.1002/eco.101.

Davis, M.B., and Ford, M.S., 1982, Sediment focusing in Mirror Lake, New Hampshire: Limnology and Oceanography, v. 27, no. 1, p. 137–150, http://dx.doi.org/10.4319/lo.1982.27.1.0137.

Dean, W.E., and Gorham, Eville, 1998, Magnitude and significance of carbon burial in lakes, reservoirs, and peatlands: Geology, v. 26, no. 6, p. 535–538, http://dx.doi.org/10.1130/0091-7613(1998)026<0535:MASOCB>2.3.CO;2.

Driscoll, C.T., Fuller, R.D., and Schecher, W.D., 1989, The role of organic acids in the acidification of surface waters in the Eastern U.S.: Water, Air, and Soil Pollution, v. 43, no. 1–2, p. 21–40, http://dx.doi.org/10.1007/BF00175580.

Dürr, H.H., Meybeck, Michel, and Dürr, S.H., 2005, Lithologic composition of the Earth's continental surfaces derived from a new digital map emphasizing riverine material transfer: Global Biogeochemical Cycles, v. 19, no. 4, article GB4S10, 22 p., http://dx.doi.org/10.1029/2005GB002515.

Efron, Bradley, and Tibshirani, R.J., 1994, An introduction to the bootstrap: Boca Raton, Fla., Chapman & Hall/CRC, Monographs on Statistics and Applied Probability, v. 57, 456 p.

Ellis, J.M., and Calkin, P.E., 1984, Chronology of Holocene glaciation, central Brooks Range, Alaska: Geological Society of America Bulletin, v. 95, no. 8, p. 897–912, http://dx.doi.org/10.1130/0016-7606(1984)95<897:COHGCB>2.0.CO;2.

Environment and Climate Change Canada, 2014, Fresh Water Quality Monitoring—Online data: Environment and Climate Change Canada, accessed October 27, 2014, at https://www.ec.gc.ca/eaudouce-freshwater/default.asp?lang=En&n=EFDA57C6-1.

Fellman, J.B., D'Amore, D.V., Hood, Eran, and Boone, R.D., 2008, Fluorescence characteristics and biodegradability of dissolved organic matter in forest and wetland soils from coastal temperate watersheds in southeast Alaska: Biogeochemistry, v. 88, no. 2, p. 169–184, http://dx.doi.org/10.1007/s10533-008-9203-x.

Ferland, M.-E., del Giorgio, P.A., Teodoru, C.R., and Prairie, Y.T., 2012, Long-term C accumulation and total C stocks in boreal lakes in northern Québec: Global Biogeochemical Cycles, v. 26, no. 4, article GB0E04, 10 p., http://dx.doi.org/10.1029/2011GB004241.

Finkenbinder, M.S., Abbott, M.B., Edwards, M.E., Langdon, C.T., Steinman, B.A., and Finney, B.P., 2014, A 31,000 year record of paleoenvironmental and lake-level change from Harding Lake, Alaska, USA: Quaternary Science Reviews, v. 87, p. 98–113, http://dx.doi.org/10.1016/j.quascirev.2014.01.005.

Finney, B.P., Bigelow, N.H., Barber, V.A., and Edwards, M.E., 2012, Holocene climate change and carbon cycling in a groundwater-fed, boreal forest lake; Dune Lake, Alaska: Journal of Paleolimnology, v. 48, no. 1, p. 43–54, http://dx.doi.org/10.1007/s10933-012-9617-2.

Frey, K.E., and McClelland, J.W., 2009, Impacts of permafrost degradation on arctic river biogeochemistry: Hydrological Processes, v. 23, no. 1, p. 169–182, http://dx.doi.org/10.1002/hyp.7196.

Frohn, R.C., Hinkel, K.M., and Eisner, W.R., 2005, Satellite remote sensing classification of thaw lakes and drained thaw lake basins on the North Slope of Alaska: Remote Sensing of Environment, v. 97, no. 1, p. 116–126, http://dx.doi.org/10.1016/j.rse.2005.04.022.

Fry, J.A., Xian, George, Jin, Suming, Dewitz, J.A., Homer, C.G., Yang, Limin, Barnes, C.A., Herold, N.D., and Wickham, J.D., 2011, Completion of the 2006 National Land Cover Database for the conterminous United States: Photogrammetric Engineering & Remote Sensing, v. 77, no. 9, p. 858–864. [Also available at http://www.mrlc.gov/nlcd2006.php.]

Hair, J.F., Black, Bill, Babin, Barry, Anderson, R.E., and Tatham, R.L., 2006, Multivariate data analysis (6th ed.): Upper Saddle River, N.J., Pearson Prentice Hall, 899 p.

Hall, R.O., Jr., Kennedy, T.A., and Rosi-Marshall, E.J., 2012, Air–water oxygen exchange in a large whitewater river: Limnology and Oceanography; Fluids and Environments, v. 2, no. 1, p. 1–11, http://dx.doi.org/10.1215/21573689-1572535.

Halm, D.R., and Griffith, Brad, 2014, Water-quality data from lakes in the Yukon Flats, Alaska, 2010–2011: U.S. Geological Survey Open-File Report 2014–1181, 6 p., http://dx.doi.org/10.3133/ofr20141181.

Halm, D.R., and Guldager, Nikki, 2013, Water-quality data of lakes and wetlands in the Yukon Flats, Alaska, 2007–2009: U.S. Geological Survey Open-File Report 2012–1208, 13 p., http://pubs.usgs.gov/of/2012/1208/.

Hamilton, T.D., 1982, A late Pleistocene glacial chronology for the southern Brooks Range; Stratigraphic record and regional significance: Geological Society of America Bulletin, v. 93, no. 8, p. 700–716, http://dx.doi.org/10.1130/0016-7606(1982)93<700:ALPGCF>2.0.CO;2.

Harris, I., Jones, P.D., Osborn, T.J., and Lister, D.H., 2014, Updated high-resolution grids of monthly climatic observations—the CRU TS3.10 dataset: International Journal of Climatology, v. 34, no. 3, p. 623–642, http://dx.doi.org/10.1002/joc.3711.

Hijmans, Robert, Cameron, Susan, Parra, Juan, Jones, Peter, and Jarvis, Andrew, 2004, The WorldClim interpolated global terrestrial climate surfaces (ver. 1.3): WorldClim dataset, accessed March 24, 2014, at http://www.worldclim.org/current.

Hinzman, L.D., Bettez, N.D., Bolton, W.R., Chapin, F.S., Dyurgerov, M.B., Fastie, C.L., Griffith, Brad, Hollister, R.D., Hope, Allen, Huntington, H.P., Jensen, A.M., Jia, G.J., Jorgenson, Torre, Kane, D.L., Klein, D.R., Kofinas, Gary, Lynch, A.H., Lloyd, A.H., McGuire, A.D., Nelson, F.E., Oechel, W.C., Osterkamp, T.E., Racine, C.H., Romanovsky, V.E., Stone, R.S., Stow, D.A., Sturm, Matthew, Tweedie, C.E., Vourlitis, G.L., Walker, M.D., Walker, D.A., Webber, P.J., Welker, J.M., Winker, K.S., and Yoshikawa, Kenji, 2005, Evidence and implications of recent climate change in northern Alaska and other Arctic regions: Climatic Change, v. 72, no. 3, p. 251–298, http://dx.doi.org/10.1007/s10584-005-5352-2.

Hobbie, J.E., and Kling, G.W., eds., 2014, Alaska's changing Arctic; Ecological consequences for tundra, streams, and lakes: New York, Oxford University Press, 321 p.

Holmes, K.W., Chadwick, O.A., and Kyriakidis, P.C., 2000, Error in a USGS 30-meter digital elevation model and its impact on terrain modeling: Journal of Hydrology, v. 233, nos. 1–4, p. 154–173, http://dx.doi.org/10.1016/S0022-1694(00)00229-8.

Hood, Eran, Fellman, Jason, Spencer, R.G.M., Hernes, P.J., Edwards, Rick, D'Amore, David, and Scott, Durelle, 2009, Glaciers as a source of ancient and labile organic matter to the marine environment: Nature, v. 462, no. 7276, p. 1044–1047, http://dx.doi.org/10.1038/nature08580.

Huotari, Jussi, Haapanala, Sami, Pumpanen, Jukka, Vesala, Timo, and Ojala, Anne, 2013, Efficient gas exchange between a boreal river and the atmosphere: Geophysical Research Letters, v. 40, no. 21, p. 5683–5686, http://dx.doi.org/10.1002/2013GL057705.

Huttunen, J.T., Alm, Jukka, Liikanen, Anu, Juutinen, Sari, Larmola, Tuula, Hammar, Taina, Silvola, Jouko, and Martikainen, P.J., 2003, Fluxes of methane, carbon dioxide and nitrous oxide in boreal lakes and potential anthropogenic effects on the aquatic greenhouse gas emissions: Chemosphere, v. 52, no. 3, p. 609–621, http://dx.doi.org/10.1016/S0045-6535(03)00243-1.

Jarvis, A., Reuter, H.I., Nelson, A., and Guevara, E., 2008, Hole-filled SRTM for the globe (ver. 4): Consortium for Spatial Information (CGIAR-CSI) SRTM 90-m database, http://srtm.csi.cgiar.org.

Jobbágy, E.G., and Jackson, R.B., 2000, The vertical distribution of soil organic carbon and its relation to climate and vegetation: Ecological Applications, v. 10, no. 2, p. 423–436, http://dx.doi.org/10.1890/1051-0761(2000)010[0423:TVDOSO]2.0.CO;2.

Johnson, Cody, Kling, George, and Giblin, Anne, 2011, Sedimentation rate, concentration of macronutrients and flux for NE14, Toolik, Dimple, Perched during summer 2009: Long Term Ecological Research Network, http://dx.doi.org/10.6073/pasta/e2db8161be27bdbdcd398b0290f63f39.

Jones, B.M., Arp, C.D., Hinkel, K.M., Beck, R.A., Schmutz, J.A., and Winston, Barry, 2009, Arctic lake physical processes and regimes with implications for winter water availability and management in the National Petroleum Reserve Alaska: Environmental Management, v. 43, no. 6, p. 1071–1084, http://dx.doi.org/10.1007/s00267-008-9241-0.

Jones, M.C., Peteet, D.M., Kurdyla, Dorothy, and Guilderson, Thomas, 2009, Climate and vegetation history from a 14,000-year peatland record, Kenai Peninsula, Alaska: Quaternary Research, v. 72, no. 2, p. 207–217, http://dx.doi.org/10.1016/j.yqres.2009.04.002.

Jonsson, A., Åberg, J., Lindroth, A., and Jansson, M., 2008, Gas transfer rate and $CO_2$ flux between an unproductive lake and the atmosphere in northern Sweden: Journal of Geophysical Research; Biogeosciences, v. 113, no. G4, article G04006, 13 p., http://dx.doi.org/10.1029/2008JG000688.

Jorgenson, M.T., and Shur, Yuri, 2007, Evolution of lakes and basins in northern Alaska and discussion of the thaw lake cycle: Journal of Geophysical Research; Earth Surface, v. 112, no. F2, article F02S17, 12 p., http://dx.doi.org/10.1029/2006JF000531.

Jorgenson, Torre, Yoshikawa, Kenji, Kanevskiy, Mikhail, Shur, Yuri, Romanovsky, Vladimir, Marchenko, Sergei, Grosse, Guido, Brown, Jerry, and Jones, Ben, 2008, Permafrost characteristics of Alaska (December 2008 update to July 2008 Ninth International Conference on Permafrost [NICOP] map): Fairbanks, Alaska, University of Alaska-Fairbanks, Institute of Northern Engineering, scale 1:7,200,000, accessed August, 1, 2014, http://permafrost.gi.alaska.edu/sites/default/files/AlaskaPermafrostMap_Front_Dec2008_Jorgenson_etal_2008.pdf.

Kasischke, E.S., Verbyla, D.L., Rupp, T.S., McGuire, A.D., Murphy, K.A., Jandt, Randi, Barnes, J.L., Hoy, E.E., Duffy, P.A., Calef, Monika, and Turetsky, M.R., 2010, Alaska's changing fire regime—Implications for the vulnerability of its boreal forests: Canadian Journal of Forest Research, v. 40, no. 7, p. 1313–1324, http://dx.doi.org/10.1139/X10-098.

Kaufman, D.S., Axford, Yarrow, Anderson, R.S., Lamoureux, S.F., Schindler, D.E., Walker, I.R., and Werner, Al, 2012, A multi-proxy record of the Last Glacial Maximum and last 14,500 years of paleoenvironmental change at Lone Spruce Pond, southwestern Alaska: Journal of Paleolimnology, v. 48, no. 1, p. 9–26, http://dx.doi.org/10.1007/s10933-012-9607-4.

Kling, G.W., Kipphut, G.W., and Miller, M.C., 1992, The flux of $CO_2$ and $CH_4$ from lakes and rivers in arctic Alaska: Hydrobiologia, v. 240, no. 1–3, p. 23–36, http://dx.doi.org/10.1007/BF00013449.

Kling, G.W., Kipphut, G.W., Miller, M.M., and O'Brien, W.J., 2000, Integration of lakes and streams in a landscape perspective; The importance of material processing on spatial patterns and temporal coherence: Freshwater Biology, v. 43, no. 3, p. 477–497, http://dx.doi.org/10.1046/j.1365-2427.2000.00515.x.

Kortelainen, Pirkko, Pajunen, Hannu, Rantakari, Miitta, and Saarnisto, Matti, 2004, A large carbon pool and small sink in boreal Holocene lake sediments: Global Change Biology, v. 10, no. 10, p. 1648–1653, http://dx.doi.org/10.1111/j.1365-2486.2004.00848.x.

Kost, J.R., Verdin, K.L., Worstell, B.B., and Kelly, G.G., 2002, Methods and tools for the development of hydrologically conditioned elevation data and derivatives for national applications, *in* 2nd Annual Conference on Watershed Modeling, Las Vegas, Nev., 2002: 12 p.

Larouche, J.R., Bowden, W.B., Giordano, Rosanna, Flinn, M.B., and Crump, B.C., 2012, Microbial biogeography of arctic streams; Exploring influences of lithology and habitat: Frontiers in Microbiology, v. 3, article 309, 9 p., http://dx.doi.org/10.3389/fmicb.2012.00309.

Larsen, A.S., and Kristenson, Heidi, 2012, Alaska Shallow Lake Monitoring Program—Limnology of Denali National Park and Preserve: Fort Collins, Colo., National Park Service, Natural Resource Data Series NPS/CAKN/NRDS–2012/410, 37 p.

Leopold, L.B., and Maddock, Thomas, Jr., 1953, The hydraulic geometry of stream channels and some physiographic implications: U.S. Geological Survey Professional Paper 252, 57 p. [Also available at http://pubs.er.usgs.gov/publication/pp252.]

Ludwig, Wolfgang, Amiotte-Suchet, Philippe, and Probst, J.-L., 1999, Enhanced chemical weathering of rocks during the last glacial maximum; A sink for atmospheric $CO_2$?: Chemical Geology, v. 159, nos. 1–4, p. 147–161, http://dx.doi.org/10.1016/S0009-2541(99)00038-8.

Lynch, J.A., Clark, J.S., Bigelow, N.H., Edwards, M.E., and Finney, B.P., 2002, Geographic and temporal variations in fire history in boreal ecosystems of Alaska: Journal of Geophysical Research; Atmospheres, v. 107, no. D1, p. FFR 8–1 to FFR 8–17, http://dx.doi.org/10.1029/2001JD000332.

Mann, D.H., Heiser, P.A., and Finney, B.P., 2002, Holocene history of the Great Kobuk Sand Dunes, northwestern Alaska: Quaternary Science Reviews, v. 21, nos. 4–6, p. 709–731, http://dx.doi.org/10.1016/S0277-3791(01)00120-2.

Mast, M.A., Manthorne, D.J., and Roth, D.A., 2010, Historical deposition of mercury and selected trace elements to high-elevation National Parks in the Western U.S. inferred from lake-sediment cores: Atmospheric Environment, v. 44, nos. 21–22, p. 2577–2586, http://dx.doi.org/10.1016/j.atmosenv.2010.04.024.

Mathis, J.T., Cross, J.N., and Bates, N.R., 2011, Coupling primary production and terrestrial runoff to ocean acidification and carbonate mineral suppression in the eastern Bering Sea: Journal of Geophysical Research; Oceans, v. 116, no. C2, article C02030, 24 p., http://dx.doi.org/10.1029/2010JC006453.

McClelland, J.W., Townsend-Small, A., Holmes, R.M., Pan, Feifei, Stieglitz, M., Khosh, M., and Peterson, B.J., 2014, River export of nutrients and organic matter from the North Slope of Alaska to the Beaufort Sea: Water Resources Research, v. 50, no. 2, p. 1823–1839, http://dx.doi.org/10.1002/2013WR014722.

McDonald, C.P., Stets, E.G., Striegl, R.G., and Butman, David, 2013, Inorganic carbon loading as a primary driver of dissolved carbon dioxide concentrations in the lakes and reservoirs of the contiguous United States: Global Biogeochemical Cycles, v. 27, no. 2, p. 285–295, http://dx.doi.org/10.1002/gbc.20032.

McKay, N.P., and Kaufman, D.S., 2009, Holocene climate and glacier variability at Hallet and Greyling Lakes, Chugach Mountains, south-central Alaska: Journal of Paleolimnology, v. 41, no. 1, p. 143–159, http://dx.doi.org/10.1007/s10933-008-9260-0.

Melching, C.S., and Flores, H.E., 1999, Reaeration equations derived from U.S. Geological Survey database: Journal of Environmental Engineering, v. 125, no. 5, p. 407–414, http://dx.doi.org/10.1061/(ASCE)0733-9372(1999)125:5(407).

Michmerhuizen, C.M., Striegl, R.G., and McDonald, M.E., 1996, Potential methane emission from north-temperate lakes following ice melt: Limnology and Oceanography, v. 41, no. 5, p. 985–991, http://dx.doi.org/10.4319/lo.1996.41.5.0985.

Mulholland, P.J., and Elwood, J.W., 1982, The role of lake and reservoir sediments as sinks in the perturbed global carbon cycle: Tellus, v. 34, no. 5, p. 490–499, http://dx.doi.org/10.1111/j.2153-3490.1982.tb01837.x.

Naidu, A.S., Finney, B.P., and Baskaran, M., 1999, $^{210}$Pb- and $^{137}$Cs-based sediment accumulation rates in inner shelves and coastal lakes of subarctic and arctic Alaska; A synthesis, *in* Bruns, P., and Hass, H.C., eds., On the determination of sediment accumulation rates: GeoResearch Forum, v. 5, p. 185–196.

National Aeronautics and Space Administration (NASA), 2014, Surface meteorology and solar energy: National Aeronautics and Space Administration, accessed June 12, 2014, at https://eosweb.larc.nasa.gov/sse/.

New, Mark, Hulme, Mike, and Jones, Phil, 1999, Representing twentieth-century space–time climate variability, part I; Development of a 1961–90 mean monthly terrestrial climatology: Journal of Climate, v. 12, no. 3, p. 829–856, http://dx.doi.org/10.1175/1520-0442(1999)012<0829:RTCSTC>2.0.CO;2.

New, Mark, Hulme, Mike, and Jones, Phil, 2000, Representing twentieth-century space–time climate variability, part II; Development of 1901–96 monthly grids of terrestrial surface climate: Journal of Climate, v. 13, no. 13, p. 2217–2238, http://dx.doi.org/10.1175/1520-0442(2000)013<2217:RTCSTC>2.0.CO;2.

Osterkamp, T.E., Viereck, L., Shur, Y., Jorgenson, M.T., Racine, C., Doyle, A., and Boone, R.D., 2000, Observations of thermokarst and its impact on boreal forests in Alaska, U.S.A.: Arctic, Antarctic, and Alpine Research, v. 32, no. 3, p. 303–315, http://dx.doi.org/10.2307/1552529.

Park, C.C., 1977, World-wide variations in hydraulic geometry exponents of stream channels; An analysis and some observations: Journal of Hydrology, v. 33, nos. 1–2, p. 133–146, http://dx.doi.org/10.1016/0022-1694(77)90103-2.

Parks, Bruce, and Madison, R.J., 1985, Estimation of selected flow and water-quality characteristics of Alaskan streams: U.S. Geological Survey Water-Resources Investigations Report 84–4247, 64 p., https://pubs.er.usgs.gov/publication/wri844247.

Parkhurst, D.L., and Appelo, C.A.J., 1999, User's guide to PHREEQC (ver. 2)—A computer program for speciation, batch-reaction, one-dimensional transport, and inverse geochemical calculations: U.S. Geological Survey Water-Resources Investigations Report 99–4259, 312 p. [Also available at http://pubs.er.usgs.gov/publication/wri994259.]

Pastick, N.J., Jorgenson, M.T., Wylie, B.K., Rose, J.R., Rigge, Matthew, and Walvoord, M.A., 2014, Spatial variability and landscape controls of near-surface permafrost within the Alaskan Yukon River Basin: Journal of Geophysical Research; Biogeosciences, v. 119, no. 6, p. 1244–1265, http://dx.doi.org/10.1002/2013JG002594.

Pastick, N.J., Rigge, Matthew, Wylie, B.K., Jorgenson, M.T., Rose, J.R., Johnson, K.D., and Ji, Lei, 2014, Distribution and landscape controls of organic layer thickness and carbon within the Alaskan Yukon River Basin: Geoderma, v. 230–231, p. 79–94, http://dx.doi.org/10.1016/j.geoderma.2014.04.008.

Patton, W.W., Jr., 1973, Reconnaissance geology of the northern Yukon-Koyukuk Province, Alaska: U.S. Geological Survey Professional Paper 774–A, 17 p. [Also available at http://pubs.er.usgs.gov/publication/pp774A.]

Patton, W.W., Jr., and Miller, T.P., 1970, Preliminary geologic investigations in the Kanuti River region, Alaska: U.S. Geological Survey Bulletin 1312–J, 10 p. [Also available at http://pubs.er.usgs.gov/publication/b1312J.]

Pebble Partnership, 2011a, Water quality—Bristol Bay drainages, chap. 9 *of* Pebble Project Environmental Baseline Document 2004 through 2008: Pebble Partnership, variously paged, http://pebbleresearch.com/download/.

Pebble Partnership, 2011b, Surface water quality—Cook Inlet drainages, chap. 33 *of* Pebble Project Environmental Baseline Document 2004 through 2008: Pebble Partnership, variously paged, http://pebbleresearch.com/download/.

Ping, C.-L., Michaelson, G.J., Jorgenson, M.T., Kimble, J.M., Epstein, Howard, Romanovsky, V.E., and Walker, D.A., 2008, High stocks of soil organic carbon in the North American Arctic region: Nature Geoscience, v. 1, no. 9, p. 615–619, http://dx.doi.org/10.1038/ngeo284.

Post, R.A., 2011, Determining lake sedimentation rates using radionuclide tracers: Iowa City, Iowa, University of Iowa, M.S. thesis, 67 p.

Powell, R.D., and Molnia, B.F., 1989, Glacimarine sedimentary processes, facies and morphology of the south-southeast Alaska shelf and fjords: Marine Geology, v. 85, nos. 2–4, p. 359–390, http://dx.doi.org/10.1016/0025-3227(89)90160-6.

PRISM Climate Group, 2004, Parameter-elevation Relationships on Independent Slopes Model (PRISM): Oregon State University, accessed June 24, 2014, at http://prism.oregonstate.edu.

R Development Core Team, 2008, R—A language and environment for statistical computing: Vienna, Austria, R Foundation for Statistical Computing, http://www.R-project.org.

Raymond, P.A., Hartmann, Jens, Lauerwald, Ronny, Sobek, Sebastian, McDonald, Cory, Hoover, Mark, Butman, David, Striegl, Robert, Mayorga, Emilio, Humborg, Christoph, Kortelainen, Pirkko, Dürr, Hans, Meybeck, Michel, Ciais, Philippe, and Guth, Peter, 2013, Global carbon dioxide emissions from inland waters: Nature, v. 503, no. 7476, p. 355–359, http://dx.doi.org/10.1038/nature12760.

Raymond, P.A., Zappa, C.J., Butman, David, Bott, T.L., Potter, Jody, Mulholland, Patrick, Laursen, A.E., McDowell, W.H., and Newbold, Denis, 2012, Scaling the gas transfer velocity and hydraulic geometry in streams and small rivers: Limnology and Oceanography; Fluids and Environments, v. 2, no. 1, p. 41–53, http://dx.doi.org/10.1215/21573689-1597669.

Riera, J.L., Schindler, J.E., and Kratz, T.K., 1999, Seasonal dynamics of carbon dioxide and methane in two clear-water lakes and two bog lakes in northern Wisconsin, U.S.A.: Canadian Journal of Fisheries and Aquatic Sciences, v. 56, no. 2, p. 265–274, http://dx.doi.org/10.1139/f98-182.

Riordan, Brian, Verbyla, David, and McGuire, A.D., 2006, Shrinking ponds in subarctic Alaska based on 1950–2002 remotely sensed images: Journal of Geophysical Research; Biogeosciences, v. 111, no. G4, article G04002, 11 p., http://dx.doi.org/10.1029/2005JG000150.

Roach, J.K., Griffith, Brad, and Verbyla, David, 2013, Landscape influences on climate-related lake shrinkage at high latitudes: Global Change Biology, v. 19, no. 7, p. 2276–2284, http://dx.doi.org/10.1111/gcb.12196.

Roehm, C.L., Prairie, Y.T., and del Giorgio, P.A., 2009, The $pCO_2$ dynamics in lakes in the boreal region of northern Québec, Canada: Global Biogeochemical Cycles, v. 23, no. 3, article GB3013, 9 p., http://dx.doi.org/10.1029/2008GB003297.

Rogers, L.A., Schindler, D.E., Lisi, P.J., Holtgrieve, G.W., Leavitt, P.R., Bunting, Lynda, Finney, B.P., Selbie, D.T., Chen, Guangjie, and Gregory-Eaves, Irene, 2013, Centennial-scale fluctuations and regional complexity characterize Pacific salmon population dynamics over the past five centuries: National Academy of Sciences Proceedings, v. 110, no. 5, p. 1750–1755, http://dx.doi.org/10.1073/pnas.1212858110.

Rohr, Melanie, 2001, Paleoenvironmental changes at treeline in central Alaska; A 6,500 year long pollen and stable isotope record: Fairbanks, Alaska, University of Alaska, M.S. thesis, 186 p.

Rouse, W.R., Douglas, M.S.V., Hecky, R.E., Hershey, A.E., Kling, G.W., Lesack, Lance, Marsh, Philip, McDonald, Michael, Nicholson, B.J., Roulet, N.T., and Smol, J.P., 1997, Effects of climate change on the freshwaters of arctic and subarctic North America: Hydrological Processes, v. 11, no. 8, p. 873–902, http://dx.doi.org/10.1002/(SICI)1099-1085(19970630)11:8<873::AID-HYP510>3.0.CO;2-6.

Rover, Jennifer, Ji, Lei, Wylie, B.K., and Tieszen, L.L., 2012, Establishing water body areal extent trends in interior Alaska from multi-temporal Landsat data: Remote Sensing Letters, v. 3, no. 7, p. 595–604, http://dx.doi.org/10.1080/01431161.2011.643507.

Runkel, R.L., Crawford, C.G., and Cohn, T.A., 2004, Load estimator (LOADEST); a FORTRAN program for estimating constituent loads in streams and rivers: U.S. Geological Survey Techniques and Methods Book 4, Chapter A5, 69 p.

Scenarios Network for Alaska and Arctic Planning (SNAP), 2014, Historical monthly temperature and precipitation and historical derived temperature products: Scenarios Network for Alaska and Arctic Planning, accessed November 28, 2014, at http://www.snap.uaf.edu/data.php.

Schroth, A.W., Crusius, John, Chever, Fanny, Bostick, B.C., and Rouxel, O.J., 2011, Glacial influence on the geochemistry of riverine iron fluxes to the Gulf of Alaska and effects of deglaciation: Geophysical Research Letters, v. 38, no. 16, letter L16605, 6 p., http://dx.doi.org/10.1029/2011GL048367.

Schuur, E.A.G., Bockheim, James, Canadell, J.G., Euskirchen, Eugenie, Field, C.B., Goryachkin, S.V., Hagemann, Stefan, Kuhry, Peter, Lafleur, P.M., Lee, Hanna, Mazhitova, Galina, Nelson, F.E., Rinke, Annette, Romanovsky, V.E., Shiklomanov, Nikolay, Tarnocai, Charles, Venevsky, Sergey, Vogel, J.G., and Zimov, S.A., 2008, Vulnerability of permafrost carbon to climate change; Implications for the global carbon cycle: BioScience, v. 58, no. 8, p. 701–714, http://dx.doi.org/10.1641/B580807.

Seaber, P.R., Kapinos, F.P., and Knapp, G.L., 1987, Hydrologic unit maps: U.S. Geological Survey Water-Supply Paper 2294, 63 p., 1 pl., scale 1:7,500,000. [Also available at http://pubs.usgs.gov/wsp/wsp2294/.]

Sepulveda-Jauregui, A., Walter Anthony, K.M., Martinez-Cruz, K., Greene, S., and Thalasso, F., 2014, Methane and carbon dioxide emissions from 40 lakes along a north–south latitudinal transect in Alaska: Biogeosciences; Discussions, v. 11, no. 9, p. 13251–13307, http://dx.doi.org/10.5194/bgd-11-13251-2014.

Shimer, Grant, 2009, Holocene vegetation and climate change at Canyon Lake, Copper River Basin, Alaska: Fairbanks, Alaska, University of Alaska, M.S. thesis, 89 p.

Smol, J.P., Wolfe, A.P., Birks, H.J.B., Douglas, M.S.V., Jones, V.J., Korhola, Atte, Pienitz, Reinhard, Rühland, Kathleen, Sorvari, Sanna, Antoniades, Dermot, Brooks, S.J., Fallu, M.-A., Hughes, Mike, Keatley, B.E., Laing, T.E., Michelutti, Neal, Nazarova, Larisa, Nyman, Marjut, Paterson, A.M., Perren, Bianca, Quinlan, Roberto, Rautio, Milla, Saulnier-Talbot, Émilie, Siitonen, Susanna, Solovieva, Nadia, and Weckström, Jan, 2005, Climate-driven regime shifts in the biological communities of arctic lakes: National Academy of Sciences Proceedings, v. 102, no. 12, p. 4397–4402, http://dx.doi.org/10.1073/pnas.0500245102.

Sobek, S., Anderson, N.J., Bernasconi, S.M., and Del Sontro, T., 2014, Low organic carbon burial efficiency in arctic lake sediments: Journal of Geophysical Research; Biogeosciences, v. 119, no. 6, p. 1231–1243, http://dx.doi.org/10.1002/2014JG002612.

Sobek, Sebastian, Durisch-Kaiser, Edith, Zurbrügg, Roland, Wongfun, Nuttakan, Wessels, Martin, Pasche, Natacha, and Wehrli, Bernhard, 2009, Organic carbon burial efficiency in lake sediments controlled by oxygen exposure time and sediment source: Limnology and Oceanography, v. 54, no. 6, p. 2243–2254, http://dx.doi.org/10.4319/lo.2009.54.6.2243.

Sobek, Sebastian, Tranvik, L.J., and Cole, J.J., 2005, Temperature independence of carbon dioxide supersaturation in global lakes: Global Biogeochemical Cycles, v. 19, no. 2, article GB2003, 10 p., http://dx.doi.org/10.1029/2004GB002264.

Solomon, C.T., Bruesewitz, D.A., Richardson, D.C., Rose, K.C., Van de Bogert, M.C., Hanson, P.C., Kratz, T.K., Larget, Bret, Adrian, Rita, Babin, B.L., Chiu, C.-Y., Hamilton, D.P., Gaiser, E.E., Hendricks, Susan, Istvánovics, Vera, Laas, Alo, O'Donnell, D.M., Pace, M.L., Ryder, Elizabeth, Staehr, P.A., Torgersen, Thomas, Vanni, M.J., Weathers, K.C., and Zhu, Guangwei, 2013, Ecosystem respiration; Drivers of daily variability and background respiration in lakes around the globe: Limnology and Oceanography, v. 58, no. 3, p. 849–866, http://dx.doi.org/10.4319/lo.2013.58.3.0849.

Strahler, A.N., 1952, Dynamic basis of geomorphology: Geological Society of America Bulletin, v. 63, no. 9, p. 923–938, http://dx.doi.org/10.1130/0016-7606(1952)63[923:DBOG]2.0.CO;2.

Striegl, R.G., Dornblaser, M.M., Aiken, G.R., Wickland, K.P., and Raymond, P.A., 2007, Carbon export and cycling by the Yukon, Tanana, and Porcupine Rivers, Alaska, 2001–2005: Water Resources Research, v. 43, no. 2, article W02411, http://dx.doi.org/10.1029/2006WR005201.

Striegl, R.G., Dornblaser, M.M., McDonald, C.P., Rover, J.R., and Stets, E.G., 2012, Carbon dioxide and methane emissions from the Yukon River system: Global Biogeochemical Cycles, v. 26, no. 4, article GB0E05, 11 p., http://dx.doi.org/10.1029/2012GB004306.

Tank, S.E., Frey, K.E., Striegl, R.G., Raymond, P.A., Holmes, R.M., McClelland, J.W., and Peterson, B.J., 2012, Landscape-level controls on dissolved carbon flux from diverse catchments of the circumboreal: Global Biogeochemical Cycles, v. 26, no. 4, article BG0E02, 15 p., http://dx.doi.org/10.1029/2012GB004299.

Tank, S.E., Raymond, P.A., Striegl, R.G., McClelland, J.W., Holmes, R.M., Fiske, G.J., and Peterson, B.J., 2012, A land-to-ocean perspective on the magnitude, source and implication of DIC flux from major Arctic rivers to the Arctic Ocean: Global Biogeochemical Cycles, v. 26, no. 4, 15 p., http://dx.doi.org/10.1029/2011GB004192.

Tape, K.D., Verbyla, David, and Welker, J.M., 2011, Twentieth century erosion in Arctic Alaska foothills; The influence of shrubs, runoff, and permafrost: Journal of Geophysical Research; Biogeosciences, v. 116, no. G4, article G04024, 11 p., http://dx.doi.org/10.1029/2011JG001795.

Tarnocai, C., Canadell, J.G., Schuur, E.A.G., Kuhry, P., Mazhitova, G., and Zimov, S., 2009, Soil organic carbon pools in the northern circumpolar permafrost region: Global Biogeochemical Cycles, v. 23, no. 2, article GB2023, 11 p., http://dx.doi.org/10.1029/2008GB003327.

Tranvik, L.J., Downing, J.A., Cotner, J.B., Loiselle, S.A., Striegl, R.G., Ballatore, T.J., Dillon, Peter, Finlay, Kerri, Fortino, Kenneth, Knoll, L.B., Kortelainen, P.L., Kutser, Tiit, Larsen, Soren, Laurion, Isabelle, Leech, D.M., McCallister, S.L., McKnight, D.M., Melack, J.M., Overholt, Erin, Porter, J.A., Prairie, Yves, Renwick, W.H., Roland, Fabio, Sherman, B.S., Schindler, D.W., Sobek, Sebastian, Tremblay, Alain, Vanni, M.J., Verschoor, A.M., von Wachenfeldt, Eddie, and Weyhenmeyer, G.A., 2009, Lakes and reservoirs as regulators of carbon cycling and climate: Limnology and Oceanography, v. 54, no. 6, part 2, p. 2298–2314, http://dx.doi.org/10.4319/lo.2009.54.6_part_2.2298.

U.S. Department of Agriculture, Natural Resource Conservation Service, 2014, U.S. general soil map (STATSGO): U.S. Department of Agriculture, Natural Resource Conservation Service, accessed October 5, 2014, at http://sdmdataaccess.nrcs.usda.gov/.

U.S. Environmental Protection Agency, 2014, STORET data warehouse: U.S. Environmental Protection Agency, accessed July 21, 2014, at http://www.epa.gov/storet/dbtop.html.

U.S. Geological Survey, 2014a, National hydrography dataset: U.S. Geological Survey database, accessed April 7, 2014, at http://nhd.usgs.gov.

U.S. Geological Survey, 2014b, National water information service: U.S. Geological Survey Web site, accessed July 7, 2014, at http://waterdata.usgs.gov/nwis.

Van Heuven, S., Pierrot, D., Rae, J.W.B., Lewis, E., and Wallace, D.W.R., 2011, MATLAB program developed for $CO_2$ system calculations; ORNL/CDIAC-105b (ver. 1.1): U.S. Department of Energy, Oak Ridge National Laboratory, Carbon Dioxide Information Analysis Center, http://dx.doi.org/10.3334/CDIAC/otg.CO2SYS_MATLAB_v1.1.

Verdin, K.L., 2000, Development of the National Elevation Dataset Hydrologic Derivatives (NED-H): Proceedings of the 20th Annual ESRI International User Conference, San Diego, Calif., July 2000, accessed January 1, 2014, at http://training.esri.com/bibliography/index.cfm?event=general.recordDetail&ID=9086.

Verdin, K.L., and Worstell, Bruce, 2008, A fully distributed implementation of mean annual streamflow regional regression equations: JAWRA Journal of the American Water Resources Association, v. 44, no. 6, p. 1537–1547, http://dx.doi.org/10.1111/j.1752-1688.2008.00258.x.

Wahrhaftig, Clyde, 1965, Physiographic divisions of Alaska: U.S. Geological Survey Professional Paper 482, 52 p. [Also available at http://pubs.er.usgs.gov/publication/pp482.]

Walter, K.M., Edwards, M.E., Grosse, G., Zimov, S.A., and Chapin, F.S., III, 2007, Thermokarst lakes as a source of atmospheric $CH_4$ during the last deglaciation: Science, v. 318, no. 5850, p. 633–636, http://dx.doi.org/10.1126/science.1142924.

Walter Anthony, K.M., Zimov, S.A., Grosse, G., Jones, M.C., Anthony, P.M., Chapin, F.S., III, Finlay, J.C., Mack, M.C., Davydov, S., Frenzel, P., and Frolking, S., 2014, A shift of thermokarst lakes from carbon sources to sinks during the Holocene epoch: Nature, v. 511, no. 7510, p. 452–456, http://dx.doi.org/10.1038/nature13560.

Walvoord, M.A., and Striegl, R.G., 2007, Increased groundwater to stream discharge from permafrost thawing in the Yukon River Basin; Potential impacts on lateral export of carbon and nitrogen: Geophysical Research Letters, v. 34, no. 12, letter L12402, 6 p., http://dx.doi.org/10.1029/2007GL030216.

Walvoord, M.A., Voss, C.I., and Wellman, T.P., 2012, Influence of permafrost distribution on groundwater flow in the context of climate-driven permafrost thaw; Example from Yukon Flats Basin, Alaska, United States: Water Resources Research, v. 48, no. 7, article W07524, 17 p., http://dx.doi.org/10.1029/2011WR011595.

Wanninkhof, Rik, 1992, Relationship between wind speed and gas exchange over the ocean: Journal of Geophysical Research; Oceans, v. 97, no. C5, p. 7373–7382, http://dx.doi.org/10.1029/92JC00188.

Webb, R.S., and Webb, Thompson, III, 1988, Rates of sediment accumulation in pollen cores from small lakes and mires of eastern North America: Quaternary Research, v. 30, no. 3, p. 284–297, http://dx.doi.org/10.1016/0033-5894(88)90004-X.

Wetzel, R.G., 2001, Limnology—Lake and river ecosystems (3d ed.): San Diego, Calif., Academic Press, 1006 p.

Wik, Martin, Varner, R.K., Walter Anthony, Katey, MacIntyre, Sally, and Bastviken, David, 2016, Climate-sensitive northern lakes and ponds are critical components of methane release: Nature Geoscience, v. 9, no. 2, p. 99–106, http://dx.doi.org/10.1038/ngeo2578.

Williams, J.R., 1962, Geologic reconnaissance of the Yukon Flats district, Alaska: U.S. Geological Survey Bulletin 1111–H, p. 289–331. [Also available at http://pubs.er.usgs.gov/publication/b1111H.]

Yu, Zicheng, Walker, K.N., Evenson, E.B., and Hajdas, Irka, 2008, Lateglacial and early Holocene climate oscillations in the Matanuska Valley, south-central Alaska: Quaternary Science Reviews, v. 27, nos. 1–2, p. 148–161, http://dx.doi.org/10.1016/j.quascirev.2007.02.020.

Zappa, C.J., McGillis, W.R., Raymond, P.A., Edson, J.B., Hintsa, E.J., Zemmelink, H.J., Dacey, J.W.H., and Ho, D.T., 2007, Environmental turbulent mixing controls on air-water gas exchange in marine and aquatic systems: Geophysical Research Letters, v. 34, no. 10, letter L10601, 6 p., http://dx.doi.org/10.1029/2006GL028790.

Zhu, Zhiliang, and Reed, B.C., eds., 2012, Baseline and projected future carbon storage and greenhouse-gas fluxes in ecosystems of the Western United States: U.S. Geological Survey Professional Paper 1797, 192 p. [Also available at http://pubs.usgs.gov/pp/1797/.]

Zhu, Zhiliang, and Reed, B.C., eds., 2014, Baseline and projected future carbon storage and greenhouse-gas fluxes in ecosystems of the Eastern United States: U.S. Geological Survey Professional Paper 1804, 204 p. [Also available at http://dx.doi.org/10.3133/pp1804.]